Geoscience Frontiers 11 (2020) 129–149

HOSTED BY

Contents lists available at ScienceDirect

Geoscience Frontiers

journal homepage: www.elsevier.com/locate/gsf

Research Paper

The Intra-Pontide ophiolites in Northern Turkey revisited: From birth to death of a Neotethyan oceanic domain

Michele Marroni [a,b,*], M. Cemal Göncüoğlu [c], Chiara Frassi [a], Kaan Sayit [c], Luca Pandolfi [a,b], Alessandro Ellero [b], Giuseppe Ottria [b]

[a] Dipartimento di Scienze della Terra, Università di Pisa, via S. Maria 53, 56126, Pisa, Italy
[b] Istituto di Geoscienze e Georisorse - CNR, Via G. Moruzzi 1, 56124, Pisa, Italy
[c] Department of Geological Engineering, Middle East Technical University, 06531 Ankara, Turkey

ARTICLE INFO

Keywords:
Intra-Pontide suture zone
Central Pontides
Northern Turkey
Ophiolites
Neotethys Ocean
Geodynamics

ABSTRACT

The Anatolian peninsula is a key location to study the central portion of the Neotethys Ocean(s) and to understand how its western and eastern branches were connected. One of the lesser known branches of the Mesozoic ocean(s) is preserved in the northern ophiolite suture zone exposed in Turkey, namely, the Intra-Pontide suture zone. It is located between the Sakarya terrane and the Eurasian margin (i.e., Istanbul-Zonguldak terrane) and consists of several metamorphic and non-metamorphic units containing ophiolites produced in supra-subduction settings from the Late Triassic to the Early Cretaceous. Ophiolites preserved in the metamorphic units recorded pervasive deformations and peak metamorphic conditions ranging from blueschist to eclogite facies. In the non-metamorphic units, the complete oceanic crust sequence is preserved in tectonic units or as olistoliths in sedimentary mélanges. Geochemical, structural, metamorphic and geochronological investigations performed on ophiolite-bearing units allowed the formulation of a new geodynamic model of the entire "life" of the Intra-Pontide oceanic basin(s). The reconstruction starts with the opening of the Intra-Pontide oceanic basins during the Late Triassic between the Sakarya and Istanbul-Zonguldak continental microplates and ends with its closure caused by two different subductions events that occurred during the upper Early Jurassic and Middle Jurassic. The continental collision between the Sakarya continental microplate and the Eurasian margin developed from the upper Early Cretaceous to the Palaeocene. The presented reconstruction is an alternative model to explain the complex and articulate geodynamic evolution that characterizes the southern margin of Eurasia during the Mesozoic era.

1. Introduction

The tectonic setting of the Anatolian peninsula in Turkey (Fig. 1) is a puzzle of amalgamated Gondwana- and Eurasia-derived continental microplates rimmed by remnants of Palaeo- and Neotethyan ophiolites ranging in age from the Late Palaeozoic to Late Mesozoic (Sengör and Yılmaz, 1981; Göncüoğlu et al., 1997; Okay and Tüysüz, 1999). This setting derived by the progressive north-eastward drift of the Gondwana fragments (Peri-Gondwanan terranes, Stampfli, 2000) resulted in a complicated sequence of openings and closures of oceanic basins and repeated events of subduction and collision of continental microplates and/or oceanic plateaux (Thuizat et al., 1981; Yalınız et al., 1996; Dilek et al., 1999; Searle and Cox, 1999; Robertson, 2002; Malpas et al., 2003; Çakır, 2009; Göncüoğlu et al., 2012; Hässig et al., 2013; Sayit et al., 2016; Frassi et al., 2018).

In north-central Turkey, the Pontide domain is represented by the Istanbul-Zonguldak and the Sakarya continental terranes and by an ophiolite-bearing suture zone, i.e., the Intra-Pontide suture zone (Fig. 1). The suture zone, located at the boundary between the two terranes, consists of a tectonic stack of high-pressure metamorphic units, supra-subduction zone ophiolites, oceanic sediments and ophiolite-bearing sedimentary mélanges that testify to the presence of a large and composite oceanic domain (i.e., Intra-Pontide Ocean, IPO) during the Mesozoic (Şengör and Yilmaz, 1981; Göncüoğlu et al., 1987, 2008; Göncüoğlu and Erendil, 1990; Yilmaz, 1990; Yilmaz et al., 1995, 1997; Okay and Tüysüz, 1999; Elmas and Yiğitbaş, 2001; Robertson and

* Corresponding author. Dipartimento di Scienze della Terra, Università di Pisa, via S. Maria, 53, 56126, Pisa, Italy.
E-mail address: marroni@dst.unipi.it (M. Marroni).
Peer-review under responsibility of China University of Geosciences (Beijing).

https://doi.org/10.1016/j.gsf.2019.05.010
Received 15 June 2018; Received in revised form 5 March 2019; Accepted 28 May 2019
Available online 8 June 2019

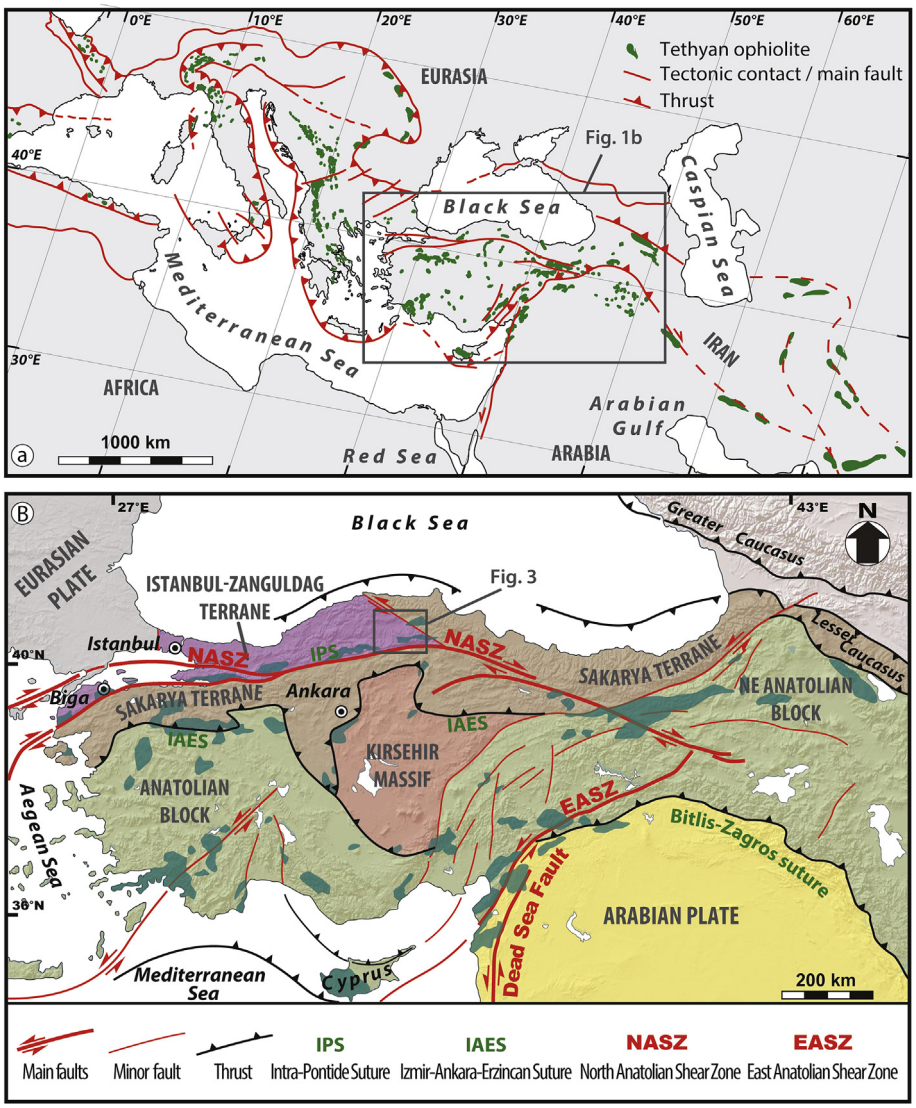

Fig. 1. (a) Tethyan ophiolites in the Mediterranean area, and (b) tectonic framework of the Anatolian peninsula and surrounding regions.

Ustaömer, 2004; Robertson et al., 2013, 2014; Marroni et al., 2014; Aygül et al., 2015, 2016; Frassi et al., 2016, 2018; Sayit et al., 2016).

Characterizing the geometrical and timing relationships that exist between the Palaeotethys and the different branches of the Neotethyan Ocean is indispensable for reconstructing the geodynamic evolution of the Eastern Mediterranean region during the Mesozoic. In this regard, we present a complete review of the lithostratigraphy, geochemistry, deformation history, metamorphism, and age data collected in the Central Pontides since 2010 by the joint research team from the Turkish Middle East Technical University of Ankara (Turkey), the Pisa University (Italy) and the Italian National Research Council. These results were published in several international papers and are combined in this paper with unpublished geochemical data to present a renewed and comprehensive geodynamics model of the Palaeotethyan and Neotethyan (i.e., IPO) oceanic domains in the Eastern Mediterranean region from the Late Palaeozoic to the Early Cretaceous.

2. Geodynamic framework of the Tethyan ophiolites in the eastern Mediterranean area

The present-day tectonic setting of the Eastern Mediterranean region is the result of a long-lived and complex interplay between continental plates and oceanic domains (including volcanic arcs) with different ages and sizes (Savostin et al., 1986; Dilek and Moores, 1990; Dilek et al., 1999; Stampfli and Borel, 2002; Stampfli and Kozur, 2006; Schmid et al., 2008; Robertson, 2012; Bortolotti et al., 2013). In this framework, a very critical time for the geodynamics of the Eastern Mediterranean region is the Mesozoic Era, during which two large oceanic areas, referred as the Palaeotethyan, opened since the Palaeozoic, and Neotethyan oceanic domains, were created and subsequently destroyed by multiple events of subduction, obduction and collision. Ophiolites derived from these wide oceanic domains are currently preserved in Turkey as tectonic units and blocks in sedimentary and/or tectonic mélanges and often imbricated with slices of continental margin deposits (Şengör and Yilmaz, 1981; Okay, 1989; Robertson, 2002; Moix et al., 2008; Okay and Whitney, 2011; Göncüoğlu et al., 2012, 2014; Plunder et al., 2013; van Hinsbergen et al., 2016; Okay et al., 2017).

The classical geodynamic reconstructions for the Eastern Mediterranean region (Stampfli and Borel, 2002; Stampfli and Kozur, 2006; Schmid et al., 2008; Robertson, 2012; Bortolotti et al., 2013) suggest that after the break-up of Pangea, a wide east-west-trending oceanic domain (i.e., the Palaeotethyan ocean) opened since the Early Permian to Triassic between the Gondwana and the Eurasian continental margins (Stampfli and Borel, 2002; Stampfli and Kozur, 2006). Its geodynamic and palaeogeographic evolution, however, is still hotly debated. The initial reconstruction (Şengör and Yilmaz, 1981) suggested that the

Palaeotethyan ocean was located north of the Sakarya microplate (i.e., south of the Eurasian plate) and was closed by southward subduction(s) (Fig. 2a). Göncüoğlu et al. (1997, 2000, 2010), Sayit et al. (2010, 2011) and Sayıt and Göncüoğlu (2009, 2013) proposed the same location but suggested that the Palaeotethyan Ocean was closed by two opposite dipping intra-oceanic subduction zones active at the end of the Triassic: a southward subduction beneath the Sakarya microplate, which created the Karakaya Complex (sensu Okay and Göncüoğlu, 2004), and a northward one that generated a supra-subduction-type complex (i.e., Küre Complex; Kozur et al., 2000). Alternative models suggest that the Palaeotethys was located to the south of the Sakarya microplate and was closed by a southward subduction (Okay et al., 1996, 2002, 2006, 2015; Okay and Tüysüz, 1999; Okay, 2000; Robertson et al., 2004; Robertson and Ustaömer, 2011, 2012; Topüz et al., 2017) (Fig. 2b) or a northward subduction (Stampfli and Borel, 2002) (Fig. 2c).

In most of the published models, the subduction event(s) leading to the closure of the Palaeotethyan Ocean produced the opening of several oceanic basins, overall referred as the Neotethyan oceanic domain (Bortolotti and Principi, 2005). This oceanic domain included three east-west trending branches represented from north to south by the IPO, the Izmir-Ankara-Erzincan Ocean and the Southern Branch of the Neothetys (or simply the Neothetys). The remains of these oceans are now preserved within the Intra-Pontide suture zone, the Izmir-Ankara-Erzincan suture zone and the Bitlis-Zagros Suture (Şengör and Yilmaz, 1981; Göncüoğlu et al., 1997; Dilek et al., 1999; Okay and Tüysüz, 1999; Parlak and Robertson, 2004) (Fig. 1b). The southernmost suture separates the Arabian plate from the Anatolide-Tauride continental microplate, whereas the Izmir-Ankara-Erzincan and the Intra-Pontide suture zones separate the Anatolide-Tauride microplate from the Sakarya microplate and the latter from the Eurasian plate, from which the Istanbul-Zonguldak terrane derived (Fig. 1b). The three suture zones contain ophiolites of various ages and geochemical signatures that record different deformation histories and metamorphic imprints. These differences imply that the Neotethyan oceanic branches opened and closed at different times by different mechanisms.

The Southern Branch of the Neotethyan Ocean opened during the Middle-Late Triassic time span (Şengör and Yilmaz, 1981; Robertson and Dixon, 1984; Göncüoğlu et al., 1987) and was consumed by two distinct intra-oceanic subductions since the early Late Cretaceous (Parlak et al., 2009; Rızaoglu et al., 2009; Çolakoglu et al., 2012; Ural et al., 2015) leading to a collision between the Arabian and the Anatolide-Tauride continental margins as late as the Miocene (Şengör et al., 2005).

Remnants of the Izmir-Ankara-Erzincan Ocean are mainly preserved in the Mersin and Ankara mélanges exposed in southern and north-central Turkey, respectively. The recent findings in the Mersin Mélange of slide-blocks of back-arc basin basalts of the late Anisian age suggests the presence of an intra-oceanic subduction zone in the Izmir-Ankara-Erzincan Ocean at least since the Middle Triassic time. As a consequence, the opening of the Izmir-Ankara-Erzincan Ocean during the Early Triassic or before (i.e., when the Palaeotethys oceanic basin was still open) is a valuable suggestion (Sayit et al., 2015, 2017). Furthermore, a mid-ocean ridge oceanic lithosphere seems to characterize the Izmir-Ankara-Erzincan Ocean in the Middle Jurassic–Early Cretaceous time span (Göncüoğlu et al., 2015; Bortolotti et al., 2018). Moreover, the occurrence of supra-subduction Tauride ophiolites of the Turonian age (Parlak et al., 2013) suggests the existence of an undeformed oceanic area that opened up to the lowermost Late Cretaceous. If the inception of the subduction deduced by the presence of back-arc basin basalts documented in the Mersin Mélange can be regarded as Middle Triassic in age, the intra-oceanic subduction within the Izmir-Ankara-Erzincan Ocean started as early as the Middle Jurassic and continued in different segments until the early Campanian (Harris et al., 1994; Önen, 2003; Çelik et al., 2018). The southward obduction of Izmir-Ankara-Erzincan ophiolites onto the Anatolide-Tauride continental margin started in the middle Maastrichtian (Göncüoğlu et al., 2003; Göncüoğlu, 2011). Remnants of the northernmost branch of the Neotethyan oceanic domain preserved within the Intra-Pontide suture zone in the Central Pontides (Northern Turkey) are the topic of this paper and will be examined in detail in the next section. Finally, at the end of the Mesozoic, the region north to the IPO was characterized by rifting (Barremian to Aptian) and spreading (from the Cenomanian to the end of the Santonian Age) leading to the opening of the back-arc basin of the Western Black Sea (Okay et al., 2013; Nikishin et al., 2015a,b).

3. Geological background of the Central Pontides

Central Pontides are located in correspondence of the arcuated sector of the North Anatolian Shear Zone (NASZ) (Şengör et al., 2005; Ellero et al., 2015a) (Figs. 1 and 3), a km-wide deformation zone where the strain is partitioned in strike-slip faults, folds and thrusts delimiting

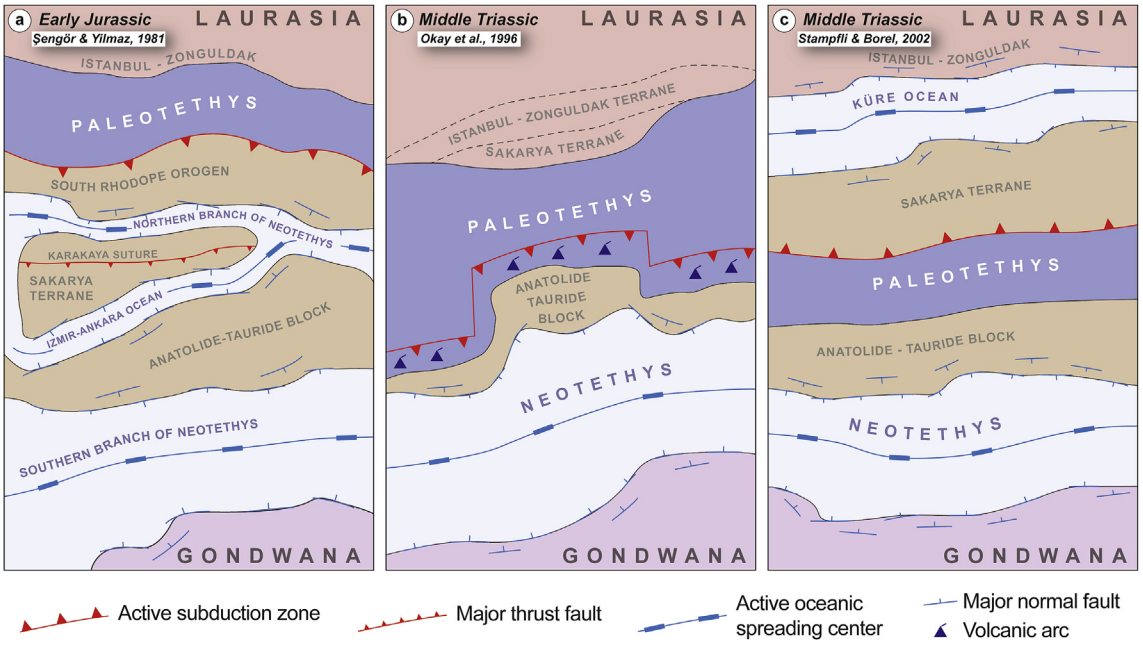

Fig. 2. Examples of the available palaeogeographic reconstructions for the Neotethyan and Palaeotethyan oceans.

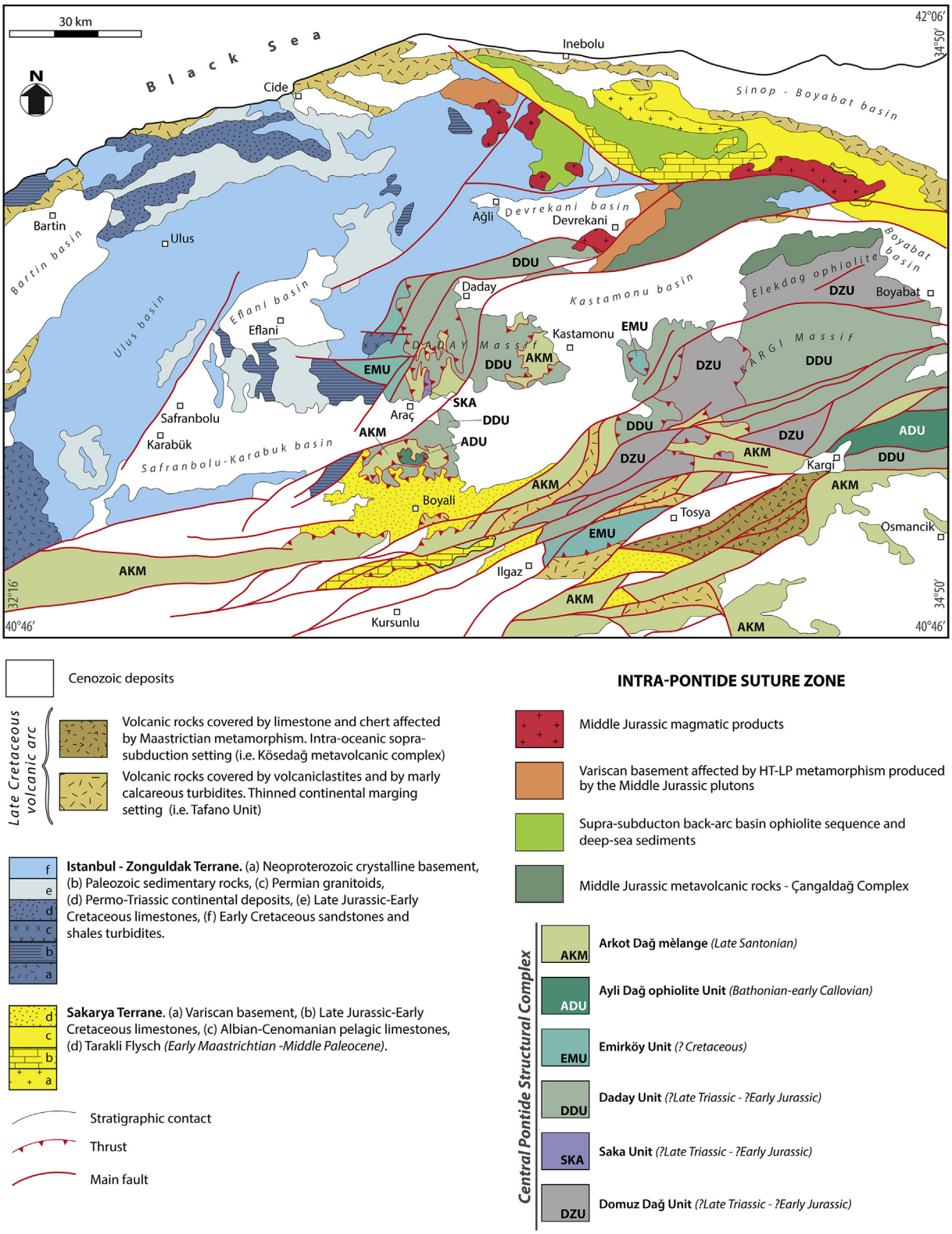

Cenozoic deposits

Late Cretaceous volcanic arc

Volcanic rocks covered by limestone and chert affected by Maastrictian metamorphism. Intra-oceanic sopra-subduction setting (i.e. Kösedağ metavolcanic complex)

Volcanic rocks covered by volcaniclastites and by marly calcareous turbidites. Thinned continental marging setting (i.e. Tafano Unit)

Istanbul - Zonguldak Terrane. (a) Neoproterozoic crystalline basement, (b) Paleozoic sedimentary rocks, (c) Permian granitoids, (d) Permo-Triassic continental deposits, (e) Late Jurassic-Early Cretaceous limestones, (f) Early Cretaceous sandstones and shales turbidites.

Sakarya Terrane. (a) Variscan basement, (b) Late Jurassic-Early Cretaceous limestones, (c) Albian-Cenomanian pelagic limestones, (d) Tarakli Flysch *(Early Maastrichtian -Middle Paleocene)*.

Stratigraphic contact

Thrust

Main fault

INTRA-PONTIDE SUTURE ZONE

Middle Jurassic magmatic products

Variscan basement affected by HT-LP metamorphism produced by the Middle Jurassic plutons

Supra-subducton back-arc basin ophiolite sequence and deep-sea sediments

Middle Jurassic metavolcanic rocks - Çangaldağ Complex

Central Pontide Structural Complex

Arkot Dağ mèlange *(Late Santonian)*

Ayli Dağ ophiolite Unit *(Bathonian-early Callovian)*

Emirköy Unit *(? Cretaceous)*

Daday Unit *(?Late Triassic - ?Early Jurassic)*

Saka Unit *(?Late Triassic - ?Early Jurassic)*

Domuz Dağ Unit *(?Late Triassic - ?Early Jurassic)*

Fig. 3. Geological sketch map of the Central Pontides (compiled from Okay et al., 2006, 2014; Hippolyte et al., 2010; Göncüoğlu et al., 2012; Marroni et al., 2014; Ellero et al., 2015a, b; Frassi et al., 2016, 2018; Sayit et al., 2017; Çelik et al., 2018).

ESE-WSW elongated blocks and pull-apart basins. The central sector of the NASZ (the Central Pontides) started since the Early Eocene (e.g. Ottria et al., 2017) and affected an imbricate stack of tectonic units consisting of metamorphic, non-metamorphic and igneous rocks ranging in age from Neo-Proterozoic to Cenozoic. The imbricate stack of the Central Pontides is the result of the Jurassic-Palaeocene closure of the IPO and the subsequent collision between two continental plates, the Sakarya microplate to the south and the Eurasian plate, today represented by the Istanbul-Zonguldak terrane to the north (Şengör and Yilmaz, 1981; Göncüoğlu et al., 1997, 2000; Okay and Tüysüz, 1999;

Akbayram et al., 2013). Even if strongly affected by the NASZ activity, the orogenic architecture produced as a consequence of the continental collision between the Sakarya and Eurasian continental margins can be defined as a tectonic stack in which the Intra-Pontide suture zone is sandwiched between the Istanbul-Zonguldak terrane, at the bottom, and the terrane, at the top. Overall, the relationships between these main orogenic elements are unconformably sealed by the post-collisional sedimentary deposits whose inception is referred to as Late Palaeocene in age (Özcan et al., 2007) (Fig. 3).

The Istanbul-Zonguldak terrane consists of a Neoproterozoic crystalline basement, which preserves evidence of Cadomian orogeny (Göncüoğlu, 2010), covered by an Early Ordovician–Late Carboniferous passive margin-type sedimentary sequence that weakly deformed during the Variscan orogeny (Görür et al., 1997; Okay and Topüz, 2017) and is locally intruded by Late Variscan (Permian) granitoids. The Palaeozoic sequences are unconformably covered by Permian to Late Triassic continental deposits (Okuyucu et al., 2017), that in turn are unconformably overlain by Late Jurassic–Early Cretaceous limestones (Aydın et al., 1995; Derman and Sayili, 1995; Tüysüz, 1999; Okay et al., 2017) that evolve upward to the Barremian-Aptian (Hippolyte et al., 2010) turbidite sequence (i.e., Çağlayan Formation) with a debris flow that mainly contains blocks of Cretaceous limestones (Okay et al., 2013).

The Intra-Pontide suture zone can instead be depicted as an imbricate stack of oceanic- and continental-derived tectonic units, each characterized by different age, metamorphic imprint, geochemistry affinity and deformation history. The remains derived from the continental margins are mainly represented by the Geme Complex and Devrekani Complex. They consist of slices of Variscan basement mainly made up of gneisses, amphibolites and marbles affected by HT-LP contact metamorphism produced by the emplacement of Middle Jurassic plutons (Okay et al., 2014; Çimen et al., 2018). Instead, the ophiolitic units derived from the IPO are represented mainly by the Central Pontides Structural Complex (Fig. 3). It consists of an imbricate stack of metamorphic and non-metamorphic units whose tectonic evolution and geodynamic significance are the main topics of this paper and whose features are described in detail in the following chapter. In addition, the Çangaldağ Metamorphic Complex is classically included in the Central Pontides Structural Complex. It includes a thick sequence of Middle Jurassic mafic to felsic metavolcanic and metavolcaniclastic rocks (Yılmaz and Bonhomme, 1991; Ustaömer and Robertson, 1999; Okay et al., 2013; Çimen et al., 2016, 2017, 2018) affected by Early Cretaceous lower greenschist facies metamorphic conditions (Yılmaz and Bonhomme, 1991; Okay et al., 2013). It is classically interpreted as a Middle Jurassic magmatic arc built on the oceanic crust of the IPO(Çimen et al., 2018).

The units exposed in the Central Pontides include the Küre Complex, a stack of slices of Early Triassic to Middle Jurassic shallow to deep-marine sedimentary cover imbricate with slices of basaltic lavas, diabases and isotropic-cumulate gabbros (Önder et al., 1987; Kozur et al., 2000; Okay et al., 2015). Its affiliation to one of the main terranes is still strongly debated (see discussion in Ustaömer and Robertson, 1999). Some authors interpreted the Küre Basin as derived from the eastern edge of the Meliata-Pindus-Maliac oceans located south of the IPO to be a Palaeotethyan supra-subduction oceanic basin (Şengör and Yilmaz, 1981; Ustaömer and Robertson, 1994; Kozur et al., 2000; Çakir et al., 2006). Other authors have regarded this complex as a Middle Jurassic back-arc basin (Küre ocean) developed on the thinned Eurasian continental margin during the slab retreat of the north-dipping Tethyan oceanic lithosphere (Alparslan and Dilek, 2017), whereas others have interpreted it as an Early Jurassic accretionary prism (Küre Complex; Çimen et al., 2018).

The Sakarya terrane includes a Variscan basement unconformably covered by a non-metamorphic continental- to shallow-marine Early Jurassic clastic rocks that are in turn unconformably topped by Middle Jurassic to Early Cretaceous neritic limestones (Altiner et al., 1991). The neritic deposits are unconformably overlain by the Albian–Cenomanian pelagic limestones showing a transition to the turbidite deposits of the Taraklı Flysch ranging in age from Late Cretaceous to Middle Palaeocene (Catanzariti et al., 2013).

Finally, the Central Pontides are characterized by several magmatic bodies produced in volcanic arc setting active during different ages (Okay et al., 2017 and references therein). Middle Jurassic arc-related magmatism produced shallow-level plutons with a dominant intermediate composition which intruded, as already mentioned, the Geme and Devrekani complexes, as well as the Küre Complex and the Çangaldağ Metamorphic Complex. Volcanic rocks from Late Cretaceous arc-related magmatism originated in two different geodynamic settings. The first is represented by an intra-oceanic supra-subduction with volcanic and sedimentary rocks characterized by Maastrichtian metamorphism (Kösedağ Metavolcanic Complex; Berber et al., 2014, 2016; Aygül et al., 2015). The second setting is represented by a volcanic arc developed on a thinned continental margin covered by volcaniclastic and sedimentary deposits (Tafano Unit and Gökçeağaç formation) (Ellero et al., 2015b; Çimen et al., 2017).

4. Ophiolite-bearing units of the Central Pontide Structural Complex in the Intra-Pontide suture zone

The Central Pontides Structural Complex (Tekin et al., 2012) comprises tectono-stratigraphic units derived from Late Triassic to Early Cretaceous fragments of oceanic lithosphere, deformed and metamorphosed during the subduction-accretion-related processes associated with the closure of the IPO (Marroni et al., 2014; Aygül et al., 2016; Çelik et al., 2016, 2018; Frassi et al., 2016, 2018; Aygül and Oberhänsli, 2017; Okay et al., 2017) (Figs. 3 and 4). Apart from the Emirköy Unit, consisting of siliciclastic turbidites and subordinate limestones recording very low-grade metamorphism facies conditions (Frassi et al., 2016), the Central Pontides Structural Complex includes five ophiolite-bearing units exposed in the Daday massif, to the west, and in the massifs located from Tosya to Kargi, to the east (Fig. 3).

In this section, we describe the state-of-the-art of lithostratigraphy, tectono-metamorphic evolution, geochemistry and age constraints of these five ophiolite-bearing units (Figs. 4–10). From higher to lower metamorphic grade, the units are: (1) the Domuz Dağ Unit (DZU) (Okay et al., 2006; Frassi et al., 2016; Sayit et al., 2016; Aygül and Oberhänsli, 2017; partly corresponding to the Bekırlı Fm. of Tüysüz and Yiğitbaş (1994); Domuzdağ-Saraycıkdağ Complex of Ustaömer and Robertson (1997)), (2) the Saka Unit (SKU) (cf. the Devrekani Unit of Marroni et al. (2014) and Saka Complex of Okay et al. (2013)) and (3) the Daday Unit (DDU) (Frassi et al., 2016, 2018; cf. Martin Complex of Okay et al. (2013)). The non-metamorphic units are the Ayli Dağ ophiolite Unit (ADU) (Göncüoğlu et al., 2012) and the Arkot Dağ Mélange (AKM) (Tokay, 1973; Göncüoğlu et al., 2014; Frassi et al., 2016, 2018; also known as Kirazbasi Mélange by Tüysüz (1990); Araç Fm. by Özcan et al. (2007) and Kirazbası Complex by Aygül et al. (2015)) (Figs. 4–6). The DZU was recognized from north of Tosya to the Kargi massif, whereas the SKU represents a small unit (less than 300 m in thickness) described exclusively in the Daday massif (Fig. 2).

The whole-rock geochemical analyses were performed at the ACME Analytical Labs (Canada) (see Table 1 in the Supplementary data). Analyses of major and most trace elements (including REE) were determined by inductively coupled plasma emission spectrometry (ICP-ES) and inductively coupled plasma mass spectrometry (ICP-MS) following a lithium borate fusion and nitric acid digestion. Ni and Pb were analysed using ICP-MS after aqua regia digestion. Analytical precision calculated based on the replicate analyses and standards indicate a reproducibility generally better than 5% for most major and trace elements.

The five ophiolite-bearing units record different polyphase tectono-metamorphic evolutions acquired at different times and structural levels during a long-lived convergence-related process (162–102 Ma: Okay et al., 2013; Marroni et al., 2014) (Figs. 4 and 10). They are characterized by different P–T paths showing different peak P–T conditions (from eclogite to blueschist facies) and exhumation paths (Fig. 10).

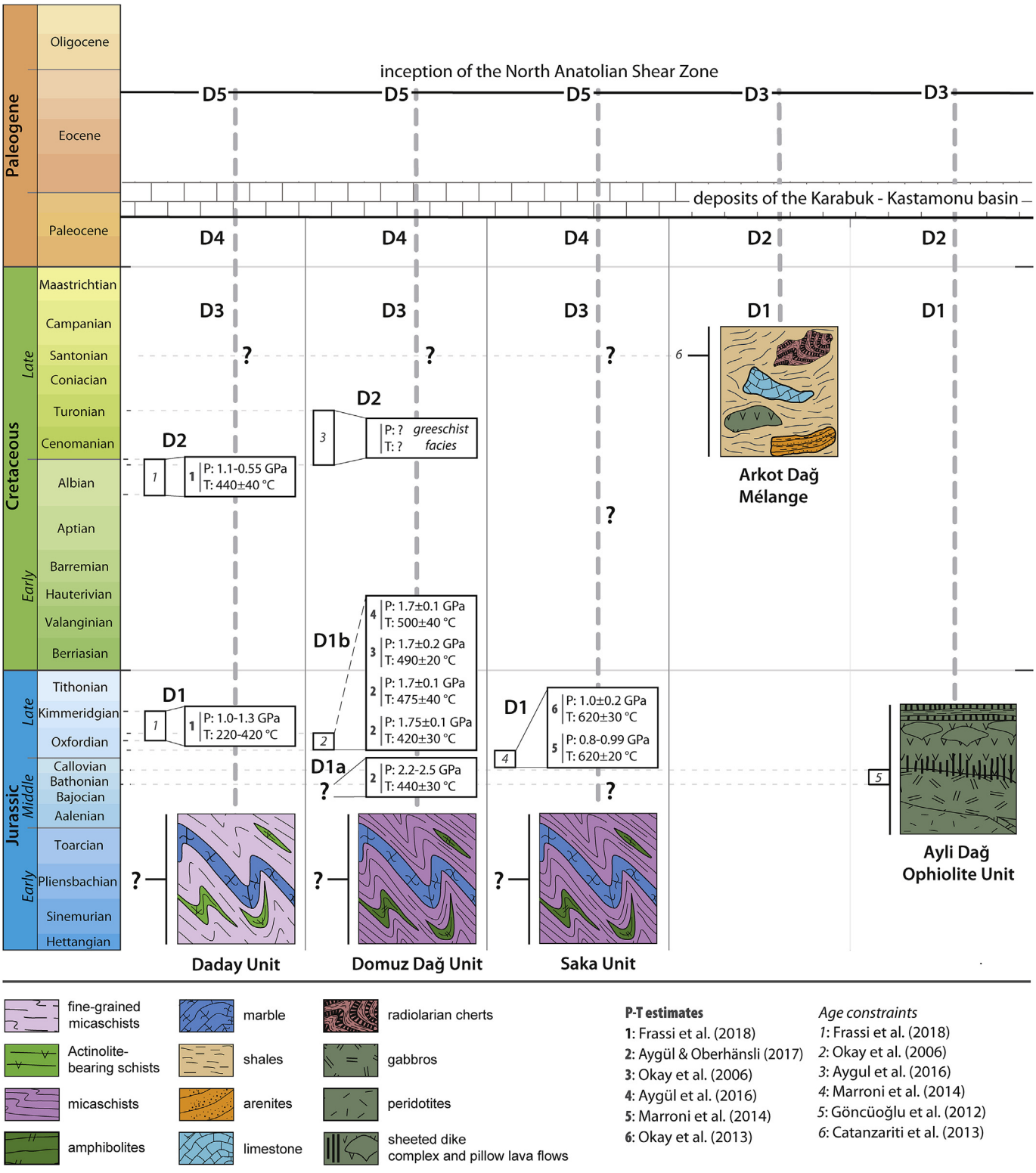

Fig. 4. Chrono-tectonic summary of the ophiolite-bearing units in the Central Pontide Structural Complex. Time scale from Cohen et al. (2013; updated, v. 2017/2).

The DZU, SKU and DDU show the more complex deformation histories recording five deformation phases (D1–D5), whereas the AKM and ADU recorded three deformation phases (D1–D3) (Fig. 4). The last three deformation phases documented in the five units of the Central Pontides Structural Complex (i.e., D3–D5 in the metamorphic units and D1–D3 in the AKU and ADU) produced comparable structures. In particular, the last documented phase (D5 phase in the metamorphic units, and D3 in the ADU and AKU) is related to the activity since the Early Eocene (Ottria et al., 2017) of the NASZ (Ellero et al., 2015a). It produced km-scale wide upright F5 folds with an ~ E–W trending axis and strike slip and/or oblique fault that affects all the tectonic contacts between units.

In the metamorphic units, the D3 and D4 phases produced structures with analogous geometry and orientations, whereas the corresponding phases in the ADU and AKU (i.e., D1 and D2) produced slightly different

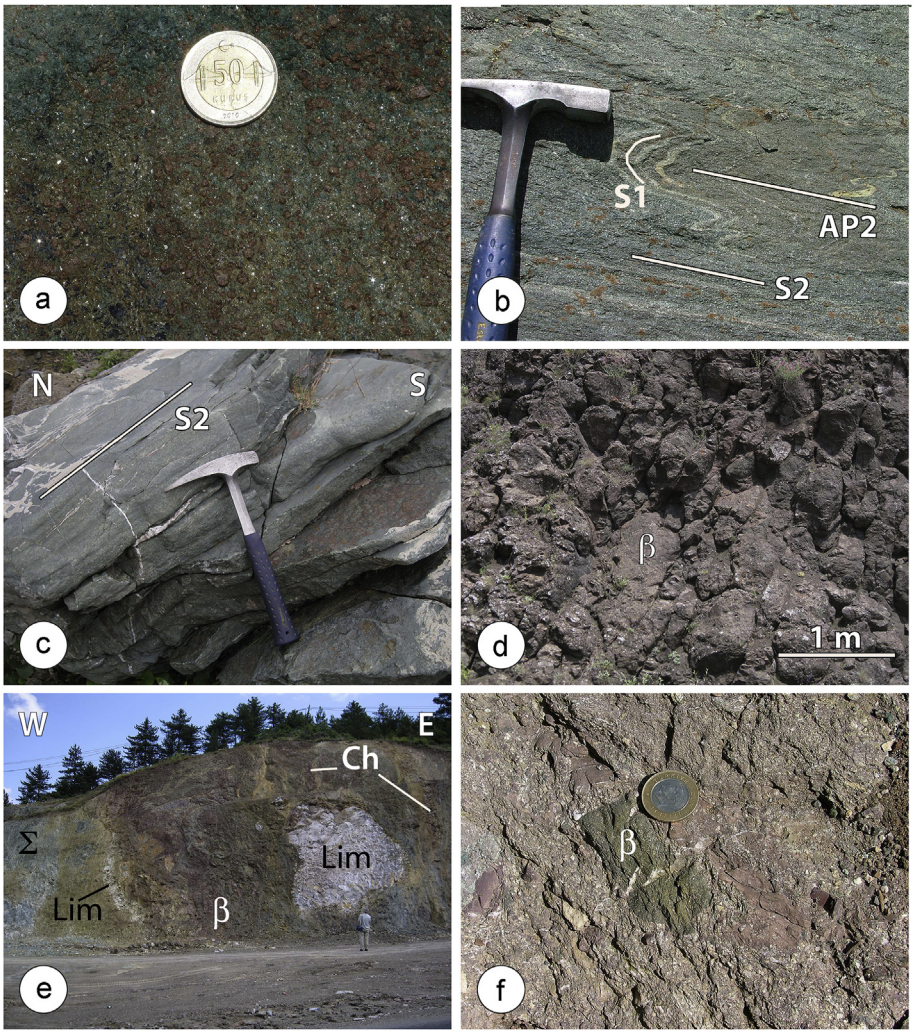

Fig. 5. Field occurrence of the representative lithologies documented in the ophiolite-bearing units in the Central Pontide Structural Complex. (a) Eclogites from the Domuz Dağ Unit north-west of Boyabat. (b) Garnet-bearing amphibolites from the Saka Unit showing relics of S1 foliation (S1) folded by the intrafoliar F2 fold (A.P. 2: F2 axial plane; S2: S2 foliation; Grt: garnet). (c) Foliated metabasites from the Daday Unit (S2: S2 foliation). (d) Pillow lavas and pillow breccias from the Ayli Dağ ophiolite Unit. (e) Spectacular exposure of the Arkot Dağ Mélange located along the Araç–Kastamonu highway (β: basalts; S: serpentinites; Lim: neritic limestone; Ch: cherts). (f) Clast of basalts (β) preserved in the Arkot Dağ Mélange.

structures (due to different rheology and structural position of these units in the Intra-Pontide suture nappe stack). For this reason, and to emphasize the different tectono-metamorphic evolutions of each unit, only the distinctive deformation phases that characterize each tectonic unit (D1 and D2 of DZU, SKU and DDU, and D1 and D2 of ADU and ARK) are described in the sections below.

To avoid repetition, the common phases documented in the metamorphic units (i.e., D3 and D4) are briefly described here. In the DZU, SKU and DDU, the D3 phase produced variably oriented close to open F3 folds, steeply inclined spaced S3 axial plane foliation, marked by phyllosilicate alignment (mainly produced by rigid body rotation) and dissolution surfaces, and a metre-thick NWN–ESE-trending thrust marked by foliated cataclasites that show a top-to-the-S sense of shear. In the same tectonic units, structures produced during the D4 phase are represented by open and parallel F4 recumbent folds with a N–S and NW–SE trending axis due to sub-horizontal disjunctive axial planes foliation (S4) and by low-angle extensional brittle shear zones (commonly associated with the F4 folds). No metamorphic blastesis occurred during the D3 and D4 phases.

4.1. Domuz Dağ Unit

4.1.1. Lithostratigraphy

The DZU consists of an assemblage of lozenge shaped slices of metamorphic rocks, mainly consisting of serpentinites, eclogites (Fig. 5a), glaucophane-bearing schists (Fig. 5b), quarzites and micaschists. The slices are generally 20–100 m thick, but the occurrence of slices of metaserpentinites with a thickness of several hundred metres also occurs and represents the main feature of this unit. The metaserpentinites are the predominant lithotypes, whereas the quarzites and micaschists are less common. This unit is characterized by lenses of coarse-grained retrogressed eclogites characterized by remnants of a high-pressure omphacite + garnet mineral assemblage. These lenses are enclosed in the metaserpentinites that are in turn surrounded by the glaucophane-bearing schists that include small slices of metaserpentinites, quarzites and micaschists. Due to severe deformation and metamorphism, any primary relationships between the different lithotypes of DZU are completely obliterated. However, all the lithotypes can be interpreted as derived by an oceanic lithosphere sequence ranging from mantle to crustal rocks including a well-developed sedimentary cover.

4.1.2. Ophiolite geochemistry

To constrain the geochemical characteristics of the DZU, we use 11 published analyses from previously study area (Sayit et al., 2016; see Supplementary Table 1) and 6 new analyses. The analysed lithologies include glaucophane-bearing schists, amphibolites, and eclogites. The metabasic rocks of the DZU are predominantly subalkaline (Nb/Y = 0.05–0.23), only one sample has an alkaline composition (Nb/Y = 3.0) (Fig. 7). Three chemical types exist in the DZU (Fig. 8). The first type is highly depleted, especially in terms of Zr and Hf (Zr_M = 0.04–0.27 and Hf_M = 0.05–0.29, where subscript M denotes "normalized to the average

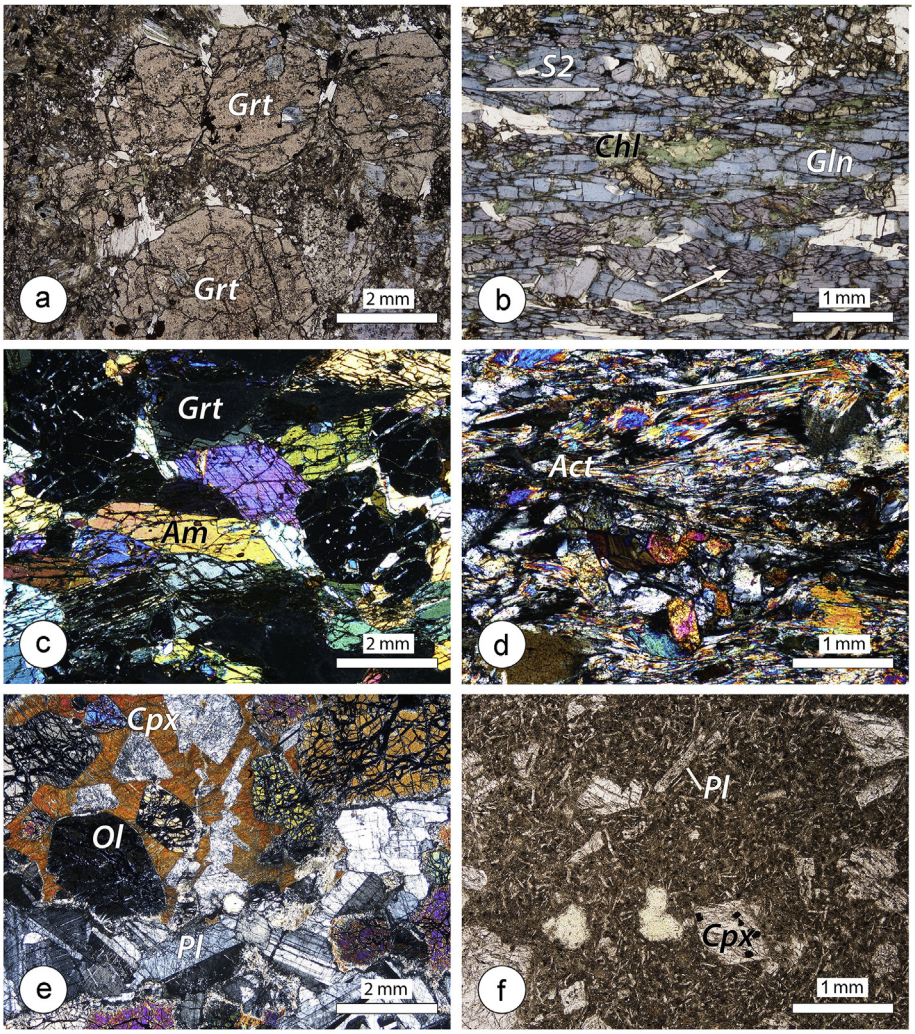

Fig. 6. Photomicrographs of the representative lithologies documented in the ophiolite-bearing units in the Central Pontide Structural Complex. (a) Eclogites from the Domuz Dağ Unit northwest of Boyabat. (b) Glaucophane-bearing schists in the Domuz Dağ Unit. (c) Coarse grained-garnet (Grt) bearing amphibolites (Am) in the Saka Unit. (d) Actinolite (Act)-bearing schists in the Daday Unit. (e) Phenocrysts of plagioclase (Pl) and clinopyroxene (Cpx) from pillow lava basalts in the Ayli Dağ ophiolite Unit. (f) Ol-gabbro in the Ayli Dağ ophiolite Unit. Abbreviations: Gln, glaucophane; Chl, chlorite; S2, S2 foliation; Ol, olivine.

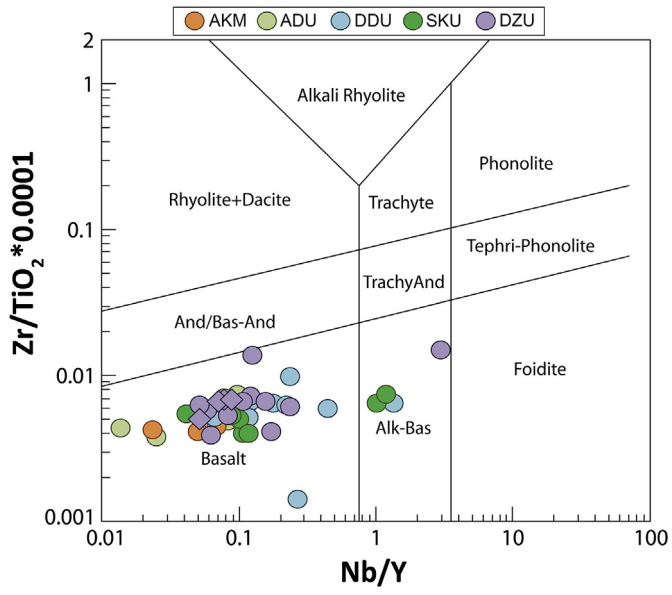

Fig. 7. Geochemical classification of the mafic rocks from the Central Pontide ophiolites (after J.A. Winchester and Floyd, 1977, modified by Pearce, 1996). AKM: Arkot Dağ Mélange; ADU: Ayli Dağ ophiolite Unit; DDU: Daday Unit; SKU: Saka Unit; DZU: Domuz Dağ Unit.

normal mid-ocean basalt (N-MORB) value of Sun and McDonough (1989)"), and akin to boninitic lavas generated at oceanic arc settings (Cameron et al., 1983). Such highly depleted compositions are also observed in the DDU and SKU (see Sections 5.2.2. and 5.3.2 below). Two samples from this chemical type are somewhat distinct from the other boninitic samples in terms of their elevated TiO_2 contents (1.6–2.0 wt.%). The second type occurs in the eastern area of the DZU, and it shows similarities to back-arc basin basalts (BABB) formed above intra-oceanic subduction zones (Leat et al., 2004). This chemical type is characterized by relatively straight to slightly fractionated HFSE patterns (Nb excluded) ($(Zr/Yb)_M = 1.0–1.7$) coupled with varying degrees of Th (and La in some cases) enrichment over Nb ($(Th/Nb)_M = 1.3–6.0$; $(La/Nb)_M = 1.2–2.6$) (Fig. 8). The BABB-type samples display a depleted to slightly enriched LREE distribution ($(La/Sm)_N = 0.7–1.8$) (Fig. 8). The third type observed in the DZU displays trace element systematics similar to those of oceanic island basalts (OIB) (Weaver et al., 1987). The OIB-type is represented by a single sample that shows significant enrichment in incompatible elements ($(Nb/Yb)_M = 55.0$) and strong LREE/HREE fractionation ($(La/Yb)_N = 27$, where subscript N denotes "chondrite-normalized, Sun and McDonough, 1989").

4.1.3. Deformation history and metamorphism

The oldest phase (D1) produced a S1 foliation rarely preserved within low-strain D2 microlithons. The P and T peak conditions of the eclogite facies metamorphism are estimated as 0.22–0.25 GPa and 440 ± 30 °C in the chloritoid micaschists by Aygül and Oberhänsli (2017). Additional

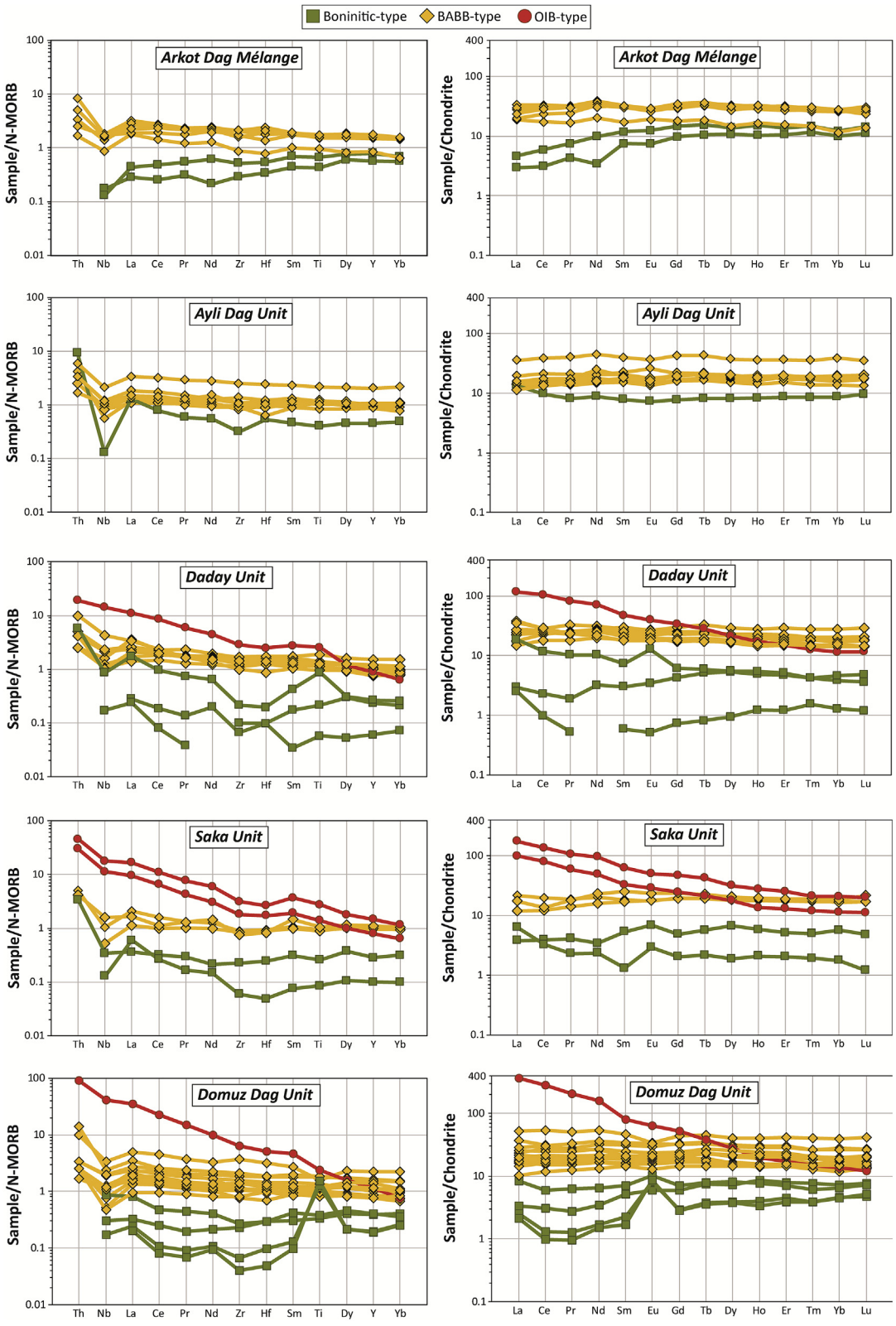

Fig. 8. Multi-element and REE patterns of the Central Pontide ophiolitic units (normalization values from Sun and McDonough, 1989).

P–T estimates constrain the blueschist facies to $P = 1.75 \pm 0.1$ GPa and $T = 420 \pm 30$ °C, and $P = 1.7 \pm 0.1$ GPa and $T = 475 \pm 40$ °C by Aygül and Oberhänsli (2017), to $P = 1.7 \pm 0.1$ GPa and $T = 500 \pm 40$ °C, and $P = 1.4 \pm 0.2$ GPa and $T = 405 \pm 35$ °C by Aygül et al. (2016) and to $P = 1.7 \pm 0.2$ GPa and $T = 490 \pm 20$ °C by Okay et al. (2006) (Figs. 4 and 10). The second deformation phase (D2) produced a continuous and penetrative foliation (S2) that represents the main structure documented in the field. It is parallel to the axial plane of intrafoliar and similar F2 folds and wraps boudins (ca. 1 m to 100 m in size) characterized by eclogite (garnet + omphacite + glaucophane + epidote + white mica) (Fig. 6a) to

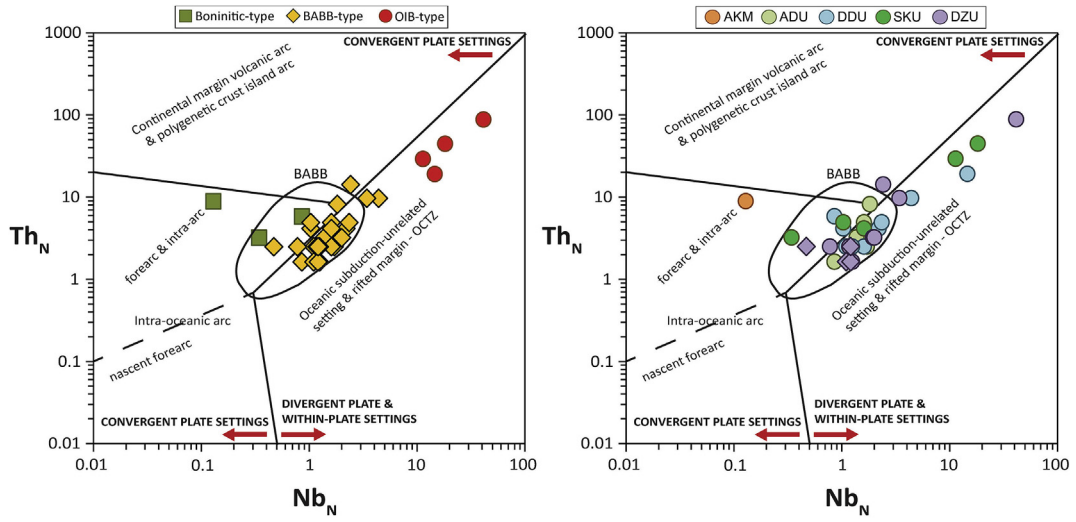

Fig. 9. Tectonomagmatic discrimination of the mafic rocks from the Central Pontide ophiolites (after Saccani, 2015). AKM: Arkot Dağ Mélange; ADU: Ayli Dağ ophiolite Unit; DDU: Daday Unit; SKU: Saka Unit; DZU: Domuz Dağ Unit.

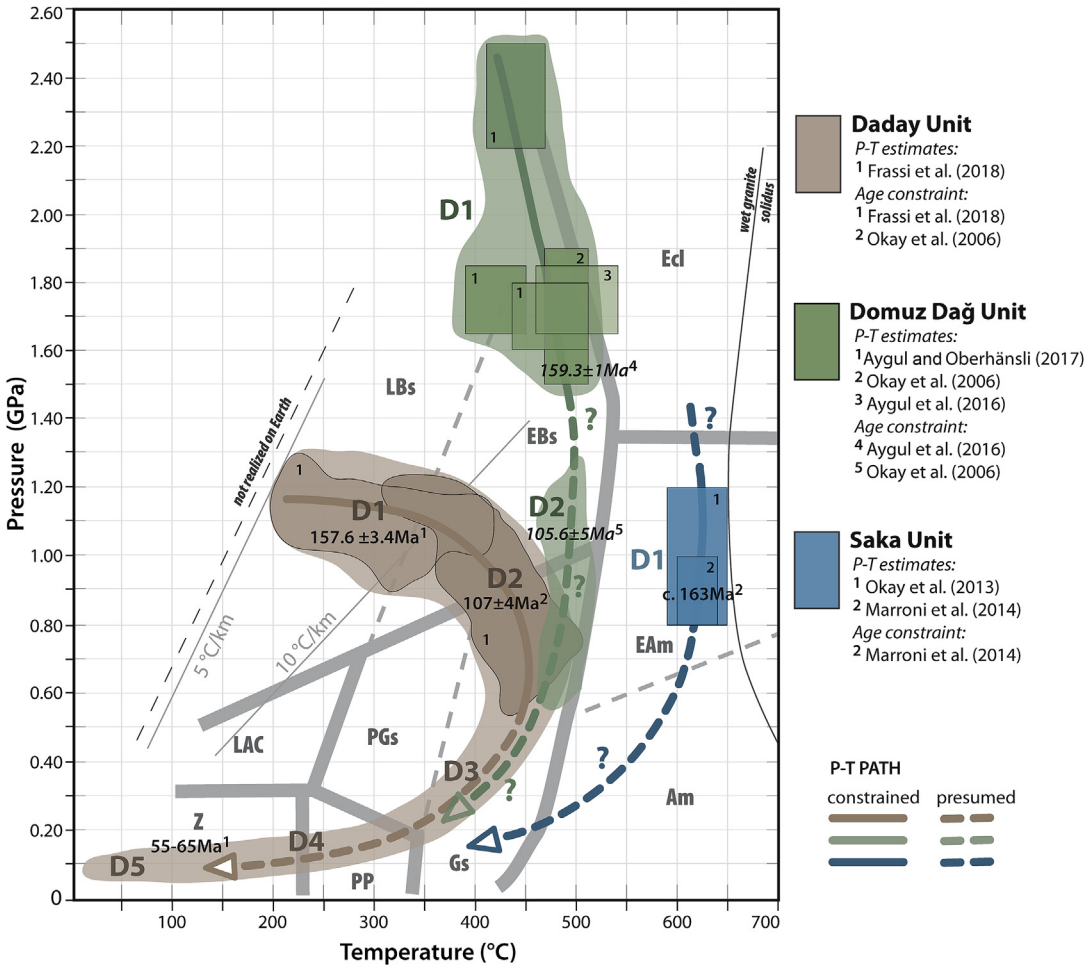

Fig. 10. Pressure-Temperature-time-deformation (P-T-d-t) paths of the ophiolite-bearing tectonic units belonging to the Intra-Pontide suture zone. Stability field of the metamorphic facies are from Frost and Frost (2013). Abbreviations: Am: amphibolite facies; EAm: epidote-amphibolite facies; Ecl: eclogite facies; EBs: epidote blueschist facies; LBs: lawsonite blueschist facies; PGs: pumpellyite greenschist facies; Gs: greenschist facies; LAC: lawsonite-albite-chlorite; PP: prehnite-pumpellyite facies; and Z: zeolite facies.

blueschist (garnet + glaucophane + epidote + chlorite + white mica ± quartz) (Fig. 6b) facies metamorphic mineral assemblages. The trend of A2 folds axes is variably oriented, whereas the S2 foliation strikes mainly NE–SW dipping less than 40° mainly towards the NW. It is defined by

quartz, plagioclase, white mica and biotite, wrapping relicts of garnet and large biotite in micaschists, and isoriented albite, epidote, chlorite and actinolite in amphibolite.

4.1.4. Age constraints

Due to the high-grade metamorphism, no palaeontological ages are available for the metasedimentary succession of the DZU. The ^{40}Ar–^{39}Ar dating of phengites from the DZU by Aygül et al. (2016) provides two different ages; the first one is 159.3 ± 1 Ma (earliest Late Jurassic), whereas the second one ranges from 100.6 ± 1.3 Ma to 91.8 ± 1.8 Ma. The two different ages can be interpreted as related, respectively, to the metamorphic peak (D1 phase) and to retrograde metamorphism during exhumation (D2 phase) (Figs. 4 and 10). In this frame, the previous ^{40}Ar–^{39}Ar age ranging between 114 Ma and 92 Ma (Aptian to Turonian) provided by Okay et al. (2006) and regarded as the age of the eclogite facies metamorphism can be thus re-interpreted as indicative of the retrograde metamorphism. The exhumation is completed before the Late Palaeocene, i.e., the oldest ages of the uppermost inter-mountain Karabük – Kastamonu Basin deposits (Özcan et al., 2007) that unconformably covered the DZU.

4.2. Saka Unit

4.2.1. Lithostratigraphy

The SKU can be described as an assemblage of up to 20 m-thick lozenge-shaped slices of amphibolites, micaschists, calcschists and impure marbles bounded by mylonitic shear zones. Amphibolites and micaschists represent the common lithotypes. Whereas the micaschists are characterized by the occurrence of coarse-grained mica and garnet crystals, the amphibolites include both coarse-grained garnet-bearing (Fig. 6c) and fine-grained garnet-free banded types (Frassi et al., 2016; Sayit et al., 2016). Primary stratigraphic relationships among the different lithotypes were strongly transposed by the polyphase deformation and metamorphism. The only remnant is represented by a decrease in micas content and increase in carbonate content moving from marbles to calcschists. As proposed for the DDU, the lithotypes of the SKU can be regarded as derived from an oceanic crustal section where basalts and gabbros are topped by cherts, limestone pelites and arenites.

4.2.2. Ophiolite geochemistry

The geochemistry of the SKU is based on 7 published whole-rock analyses of amphibolites from the Araç area (Sayit et al., 2016; see Supplementary Table 1). The mafic metamorphics of SKU have tholeiitic to alkaline compositions (Nb/Y = 0.04–1.19) (Fig. 7). Within the SKU, boninitic-, BABB- and OIB-types exist (Fig. 8), which are similar to those observed in the DZU. The boninitic samples are characterized by Zr_M and Hf_M values between 0.06–0.23 and 0.05–0.24, respectively, and by low REE abundances (Sm_N = 1.3–5.4) (Fig. 8). Regarding the BABB-type samples, the level of Th enrichment over Nb ($(Th/Nb)_M$ = 2.6–4.9) appears to occur within a narrower range compared to those from the DZU, although the La enrichment is rather similar ($(La/Nb)_M$ = 1.0–2.2). The LREE patterns in this type are depleted to slightly enriched ($(La/Sm)_N$ = 0.7–1.2) (Fig. 8). The OIB-type samples are highly enriched in incompatible elements ($(Nb/Yb)_M$ = 15.4–17.7) (Fig. 8), although the level of enrichment is lower than those from the DZU (see Section 4.1.2.).

4.2.3. Deformation history and metamorphism

The structures produced during the first deformation phase (D1) were rarely documented within low-strain domains of the D2 phase. The second deformation phase (D2) produced the most widespread structures detected both at the meso- and microscopic scale. The results show strong partitioning in the folding and shearing domains. The inverse top-to-the south shear zones delimit the units and different lithotypes. In the rock volume delimited by the D2 shear zones, similar and isoclinal F2 folds are associated with a continuous and penetrative S2 axial plane foliation. It is variably oriented and shows moderate to deep inclination mainly towards the east. In the micaschist, the S2 foliation is defined by quartz, plagioclase (An% = 0.31), garnet ($Alm_{57–63}$, $Py_{18–24}$, $Grs_{11–17}$, $Sps_{3–4}$), white micas (Si = 3.16–3.21 a.p.f.u.) ± biotite (Ti = 0.13–0.15 a.p.f.u.; X_{Mg} = 0.58–0.69) (Frassi et al., 2018). In the coarse-grained amphibolites, S2 foliation is marked by oriented brown hornblende (tschermakite), garnet ($Alm_{53–55}$, $Py_{10–19}$, $Grs_{20–24}$, $Sps_{5–7}$) and biotite crystals, whereas in the fine-grained banded amphibolites, the foliation is marked by elongated green hornblende (tschermakite to pargasite), biotite, quartz and feldspar (An% = 0.19–0.24) (Fig. 6c).

Okay et al. (2013) reported *P*–*T* conditions of 1.00 ± 0.20 GPa and 620 ± 30 °C (epidote-amphibolite facies) for the peak metamorphism during the D1 deformation phase in the amphibolite and micaschists. Classical thermobarometry applied to the same lithotypes suggest that during the D2 deformation phase the SKU was affected by a temperature of approximately 620 ± 20 °C and pressure of approximately 0.80–0.99 GPa (Marroni et al., 2014). These metamorphic conditions suggest that the accretion of the Saka Unit took place under a relatively high thermal gradient, which is uncommon for a subduction zone. However, high thermal gradients are reported in several fossil subduction complexes as a result of the subduction of a seamount or a spreading ridge (Zhang and Jin, 2016).

4.2.4. Age constraints

Due to the high-grade metamorphism, no palaeontological ages are available for the metasedimentary succession of the SKU. The metamorphic peak occurred during the uppermost Middle Jurassic time based on the ages of 163.1 ± 1.0 Ma and 163.8 ± 1.1 Ma of muscovite and biotite ^{40}Ar–^{39}Ar dating, respectively (Marroni et al., 2014) (Figs. 4 and 10). No dating is available for the retrograde metamorphism. The exhumation is completed before the Late Palaeocene, i.e., the oldest ages of the inter-mountain Karabük – Kastamonu Basin deposits (Özcan et al., 2007) that unconformably covered the SKU (Fig. 10).

4.3. Daday Unit

4.3.1. Lithostratigraphy

Like the previous tectonic units, the DDU is characterized by an assemblage of m- to dm-thick, lozenge-shaped tectonic slices separated by highly deformed shear bands (Okay et al., 2013; Frassi et al., 2016, 2018). The slices are mainly represented by fine-grained micaschists (Fig. 5c), fine- to coarse-grained paragneisses, and impure marbles. Actinolite-bearing schists and quarzites have also been found (Okay et al., 2013; Frassi et al., 2016, 2018; Sayit et al., 2016).

Although the pristine relationships between the different metasedimentary lithotypes cannot be clearly reconstructed, the interfingering relationships between the micaschists and paragneisses and the contact between actinolite-bearing schists and quarzites probably represent relicts of their primary stratigraphic association. These observations suggest that the rocks of the DDU derive from an oceanic crustal section including basic volcanic rocks of oceanic crust origin topped by cherts and limestones grading upwards into shales and arenites that probably represent turbiditic deposits (Frassi et al., 2016, 2018).

4.3.2. Ophiolite geochemistry

The geochemistry of the DDU is based on the published whole-rock analyses of a total of 11 samples from the Araç and Emirköy areas (Sayit et al., 2016; see Supplementary Table 1). The analysed lithologies include greenschist facies metabasaltic and metagabbroic rocks. The DDU consists of metabasic rocks with a predominantly tholeiitic character, except for one sample that possess alkaline compositions (Nb/Y = 0.07–1.34) (Fig. 7). Trace element systematics reveals three major chemical species (boninitic-, BABB- and OIB-type) within the DDU (Fig. 7). The boninitic type is highly depleted with very low abundances of Zr, Hf and REE (Zr_M = 0.07–0.22; Hf_M = 0.1–0.2; Sm_N = 0.6–7.3) (Fig. 8). The BABB-type shows relative enrichment in Th and La to varying extents ($(Th/Nb)_M$ = 1.6–4.0; $(La/Nb)_M$ = 0.8–2.3), coupled

with relatively straight to slightly fractionated HFSE patterns (Nb excluded) ($(Zr/Yb)_M = 1.1–1.7$) (Fig. 8). They display depleted to slightly enriched LREE distributions ($(La/Sm)_N = 0.6–2.0$). The OIB-type, which is represented by a single sample, shows significant enrichment in incompatible elements ($(Nb/Yb)_M = 22.4$) and strong LREE/HREE fractionation ($(La/Yb)_N = 10.2$).

4.3.3. Deformation history and metamorphism

S1 continuous foliation, the oldest structural element documented in the field, is highlighted by the syn-kinematic growth of quartz + phengite + chlorite ± albite and by hornblende + plagioclase + phengite + chlorite ± biotite, in the metasediments and in the metabasites, respectively (Frassi et al., 2018). The second deformation phase (D2) produced the main structures documented in the field. It is partitioned in sheared and folded domains. The formers, with a top-to-the south sense of shear, are localized at the boundaries between the different lithotypes, whereas the folded domains are preserved within each slice. There, the D2 phase produces isoclinal F2 folds and continuous S2 axial plane foliation highlighted by the syn-kinematic growth of quartz + phengite + chlorite ± albite ± calcite ± rutile (±chloritoid) in metasediments, and of chlorite + phengite + actinolite + quartz + albite + epidote ± ilmenite, in metabasites (Fig. 6d).

The P-T-d path of the DDU (Frassi et al., 2018) defines a clockwise trajectory in which the unit was buried under blueschist facies conditions at a depth of ~35–44 km (D1 phase; $T = 220–420$ °C, $P = 1.0–1.3$ GPa) and then exhumed during progressive top-to-the-S shearing from deep (~37–17 km; D2 phase: $T = 400–480$ °C, $P = 0.55–1.1$ GPa) to shallow crustal levels (<15 km of depth; D3 phase) (Fig. 10).

4.3.4. Age constraints

Even if no palaeontological ages are available for the metasedimentary succession of the DDU, its deposition age can be inferred as not older than the Early Jurassic based on the findings in the meta-arenites of detrital zircons of the Early Jurassic age (Okay et al., 2013). According to Frassi et al. (2018), the D1 phase occurred during the lowermost Late Jurassic ($^{40}Ar–^{39}Ar$ on white mica: 157.6 ± 3.4 Ma) (Figs. 4 and 10). The age of the D2 phase can be assigned to Albian (107 ± 4 Ma) by the $^{40}Ar–^{39}Ar$ ages provided by Okay et al. (2013) for fine-grained white micas grown along the pervasive S2 foliation (Figs. 4 and 5). In the same way, the ages of 101.5 ± 4.8 Ma and 99.9 ± 1.7 Ma (Albian to Cenomanian) provided by Aygül et al. (2016) by $^{40}Ar–^{39}Ar$ dating can be regarded as related to the D2 phase. In addition, the final stage of uplift of the DDU is constrained by the AFT ages of ~58 Ma (Late Palaeocene) provided by Frassi et al. (2018) (Figs. 4 and 10). This dating is coherent with the unconformable relationship between the DDU and the deposits of the inter-mountain Karabük – Kastamonu Basin, whose sedimentation started in the Late Palaeocene (Özcan et al., 2007).

4.4. Ayli Dağ ophiolite unit

4.4.1. Lithostratigraphy

The ADU is mainly represented by slices of mantle peridotites, but in the Ayli Dağ area, a complete ophiolite sequence can be reconstructed in detail (Göncüoğlu et al., 2012). Within the mantle section, pyroxenite and dunite bands, as well as dykes of rodingites and dolerites, have been identified. The mantle section is topped by 400 m-thick layered gabbros showing alternating, dm- to m-thick layers of spinel-bearing dunites, melatroctolites and troctolites. The layered gabbros show a transition to 150–200 m thick isotropic gabbros made up of Ol-gabbros (Fig. 6e) and leucogabbros with a medium to coarse-grained texture. The sequence is interrupted by a fault that hampers any observation of the uppermost levels of the intrusive complex, but beyond the fault, a sheeted dyke complex has been identified. The sheeted dyke complex, showing a thickness not more than 150 m, consists of a network of dykes with different colours, textures and grains. At the top of the sheeted dyke complex, 100–200 m-thick massive basalts, characterized by a well-developed fine to medium grained holocrystalline texture, occur. The massive basalts grade to a 400–500 m-thick sequence of pillow lavas basalts (Figs. 5d and 6f) alternating with ophiolite-bearing sandstones, siliceous mudstones and cherts.

4.4.2. Ophiolite geochemistry

Eight published whole-rock geochemical data (Göncüoğlu et al., 2012; see Supplementary Table 1) from basalts suggest that the ADU has an entirely subalkaline character ($Nb/Y = 0.01–0.10$) (Fig. 7). The studied ADU samples show boninitic and BABB-type geochemical signatures (Fig. 8). The boninitic-type exhibit low Zr and Hf abundances ($Zr_M = 0.29–0.52$ and $Hf_M = 0.34–0.54$), but slightly higher than the other boninitic samples documented in the previous units. Nb, however, is highly depleted in the ADU boninitic samples ($Nb_M = 0.13–17$). Regarding the BABB-type samples, they are mostly characterized by strong Th-La enrichment over Nb ($(Th/Nb)_M = 1.5–4.6$, $(La/Nb)_M = 1.1–2.1$) (Fig. 8). In addition, they exhibit depleted to slight LREE signatures ($(La/Sm)_N = 0.7–1.1$).

4.4.3. Deformation history

The ophiolite sequence of the ADU is characterized by the complete lack of orogenic-related metamorphism. The first phase (D1) produced thrusts with a top-to-the south sense of shear. They are localized at the boundaries of the units and are frequently bounded by hundred m-thick slices of serpentinized peridotites. During the second deformation phase (D2), D1 thrusts were reactivated as a brittle low-angle normal fault.

4.4.4. Age constraints

The radiolarian cherts at the top of the pillow lava sequence of the Ayli Dağ area have provided several taxa that indicate a depositional age of the middle Bathonian to early Callovian (uppermost Middle Jurassic) (Göncüoğlu et al., 2012) (Fig. 4). Moreover, a Late Jurassic age for the cherts at the top of basalts has been determined in the western areas of the Intra-Pontide suture zone (Göncüoğlu et al., 2008).

The age of the deformation of the ADU is not well constrained. According to the regional geological setting, the ophiolite sequence has been deformed and emplaced on the Sakarya domain before the Late Palaeocene deposition of the inter-mountain Karabük–Kastamonu Basin deposits (Özcan et al., 2007). In addition, the occurrence of ophiolites with the same ages and the same geochemical signature as slide blocks in the late Santonian AKM can be interpreted as evidence that the deformation of the domain from which the ADU derived had already started in the Late Cretaceous.

4.5. Arkot Dağ mélange

4.5.1. Lithostratigraphy

The AKM is a sedimentary mélange, not thicker than 1000 m, showing a typical block-in matrix texture (Göncüoğlu et al., 2014) (Fig. 5e and f). It consists of an assemblage of slide-blocks with different sizes and lithologies with a thickness ranging from 2–3 m to 30–40 m and width from 5–10 m to 500 m. The sedimentary matrix is scarce or even completely absent.

The slide blocks derived from different sources ranging from metamorphic continental basement (mainly micaschists and gneisses), to oceanic lithosphere (peridotites, gabbros, basalts and cherts) (Fig. 5e and f) to sedimentary rocks (limestone, marly limestone and ophiolite-bearing turbidites). Cherts often preserve primary relationships with basaltic rocks (Göncüoğlu et al., 2008, 2014). Even if most of the slide-blocks are bounded by brittle shear zones, primary sedimentary relationships between slide blocks and matrix were locally documented. The matrix consists of shales, coarse-grained arenites, pebbly mudstones and pebbly sandstones derived from the same sources as the oceanic and/or continental sequences recognized in the slide-blocks. The facies association of the mélange matrix indicates that it was probably deposited as submarine landslides active along steep slopes.

In the Late Cretaceous Kızılırmak Mèlange (Çelik et al., 2016), which can be correlated with the AKM, the lithotypes of slide blocks are similar with those of the AKM (i.e., serpentinites, basalts, gabbros, radioliarian cherts and mudstones) with the exception of metabasites not yet documented in the AKM. The metabasites in the Kızılırmak Mèlange show a mineral assemblage suggesting a metamorphic peak at a temperature higher than 700 °C and pressure of 0.5–0.6 GPa.

4.5.2. Ophiolite geochemistry

Based on the 8 published whole-rock geochemical data from the Araç and Emirköy areas (Göncüoğlu et al., 2014; Sayit et al., 2016; see Supplementary Table 1), the AKM includes subalkaline basalts and greenschists (Nb/Y = 0.02–0.10; Fig. 7) with boninitic and BABB-type geochemical signatures (Fig. 8). The boninitic-type is characterized by a single sample from the Araç area, which display strong depletion in Nb and Zr (Nb_M = 0.13 and Zr_M = 0.32) (Fig. 7). The BABB-type samples come from both the Araç and Tosya areas, and they mostly exhibit negative Nb anomalies ($(Th/Nb)_M$ = 1.6–7.5, $(La/Nb)_M$ = 1.3–2.2), coupled with depleted to flat LREE signatures ($(La/Sm)_N$ = 0.6–1.0) (Fig. 8).

4.5.3. Deformation history

The oldest deformation phase (D1; Fig. 4) is strongly partitioned and produced brittle-ductile shear zones (1–50 m thick) with a top-to-the south sense of shear. They are localized at the boundary of the AKM slices and around the biggest mélange blocks. At the microscopic scale, the S1 foliation is marked by surfaces of dissolution around calcite, quartz and basalt fragments. Deformation twins in calcite crystals suggest a possible deformation temperature of 150–300 °C (Göncüoğlu et al., 2014). The D2 phase, rarely documented, reactivated D1 thrusts as extensional faults.

4.5.4. Age constraints

The AKM can be regarded as late Santonian in age according to the nannofossil assemblage found in the soft clasts of marls detected in the matrix (Göncüoğlu et al., 2014) (Fig. 4). Cherts show a wide range of ages from the earliest Middle Triassic to earliest Late Cretaceous (Göncüoğlu et al., 2008, 2014). The oldest ones clearly indicate that the deep-water condition had already occurred by the Middle Triassic (Göncüoğlu et al., 2008, 2014), whereas the original stratigraphic relationship between early Bajocian–early Kimmeridgian cherts and basaltic breccia indicates the presence of a wide oceanic basin during the Middle-Late Jurassic. In addition, recent ^{40}Ar–^{39}Ar hornblende datings provided by Çelik et al. (2016) indicate ages ranging from 159.4 ± 0.4 Ma to 163.5 ± 0.8 Ma (Late Jurassic) for the slide blocks of high-grade metabasite. According to these ages, these rocks can be regarded as derived from the metamorphic units of the Intra-Pontide suture zone (cf. SKU), which indicates these units were reworked in the Late Cretaceous sedimentary mélanges.

The age of the deformation of the AKM is constrained by the unconformable relationships with the Late Palaeocene deposits of the inter-mountain Karabük-Kastamonu Basin (Özcan et al., 2007). Thus, the deformation of this mélange is bracketed between the Late Cretaceous and Late Palaeocene.

5. Discussion

A review of the available data about the Intra-Pontide suture zone is performed to propose a new picture of the geodynamic evolution of the Intra-Pontide domain, from the opening to the closure of the IPO basin and the subsequent collision between the Sakarya and Istanbul-Zonguldak continental margins. This reconstruction is proposed for a time span running from the Triassic to Late Cretaceous.

5.1. Petrogenetic significance of the Intra-Pontide suture zone ophiolites

Trace element systematics performed on metabasic rocks collected in the ophiolite-bearing units described in Section 4 reveal the occurrence of three main chemical types (Fig. 8). These distinct signatures appear to have developed due to involvement of heterogeneous mantle sources and subduction-related metasomatic events in the petrogenesis of the protoliths (e.g., basalts and gabbros) of the studied units. Of the chemical types observed within the five studied units, the boninitic type (found in all units – i.e., AKM, ADU, DDU, SKU, DZU; Fig. 8) is the most depleted one as evidenced by the very low abundances of Zr and Hf (Zr_M = 0.04–0.52 and Hf_M = 0.05– 0.54). The OIB-type (found in DDU, SKU, DZU; Figs. 8 and 9), on the other hand, is the most enriched with highly elevated concentrations in very incompatible trace elements (Th_M = 19.2–89.2 and Nb_M = 11.3–41.5). The BABB-type (found in all units; Fig. 8) remains between these two extremes.

The depleted concentrations of HFSE observed in boninitic, and some BABB-type samples can be attributed to predominant involvement of depleted mantle sources in their origin (e.g., N-MORB source mantle). The highly enriched incompatible element budget of the OIB-type, on the other hand, calls for significant contribution from enriched mantle sources. The mildly enriched contents, which are encountered in some portion of the BABB-type, can be attributed to involvement of both depleted and enriched mantle sources. All these varying source contributions can be explained within a framework involving a heterogeneous mantle source composed of both depleted and enriched domains.

In a heterogeneous mantle source, the depleted domain can be envisioned to be the matrix, whereas the enriched domains are found as streaks embedded in this matrix (Allègre and Turcotte, 1986; Zindler and Hart, 1986). The matrix therefore represents the depleted mantle, and lithologically, it is made up of volatile-free peridotite. The enriched streaks, on the other hand, can generally be assumed to be recycled oceanic lithosphere (Sun and McDonough, 1989; Pilet et al., 2005; Sayit, 2013). In this context, boninitic, and some BABB-type samples represent melts mostly derived from the depleted peridotite. However, it is also important to note that these samples mostly contain a subduction component that is reflected by the relative Th-La enrichment over Nb. This requires a mantle source region metasomatized by slab-derived fluids/melts (Pearce and Peate, 1995).

In addition, it is worth to noting that boninitic and some BABB-type samples display HFSE abundances lower than those of N-MORB (especially boninitic more than BABB-type). This situation cannot be readily explained by direct involvement of a typical N-MORB source but requires even more depleted sources in their petrogenesis. Therefore, a mantle source that has experienced a previous melt extraction (i.e., pre-depleted mantle source) appears to be necessary for the genesis of these chemical types. It must be noted, however, that extreme depletion observed in some boninitic samples from the DZU can be partly attributed to a cumulate origin as reflected by its strong positive Ti anomalies. In contrast to the depleted samples, the OIB-type reflects partial melts that originated chiefly from the easily fusible enriched oceanic lithosphere.

The presence of distinct geochemical signatures documented in the metabasic rocks of the Central Pontides Structural Complex can be explained by a relatively simple model involving an arc-basin system. The highly depleted characteristics of boninitic type are typically found in lavas created in the forearc region of oceanic arcs (i.e., boninites; Cameron et al., 1983; Bedard, 1999) (Fig. 9). The BABB-type reflects the variable involvement of the subduction component for most samples. The HFSE concentrations in this type are generally similar to that of N-MORB, whereas a minor amount displays slight enrichment or depletion. Such features are found in magmas generated in oceanic back-arcs (Fretzdorff et al., 2002) (Fig. 9).

While most BABB-type samples have involved a subduction-related input, just a few samples lack a clear subduction signature. This latter group of samples display a trace element distribution similar to or slightly enriched compared with N-MORB. For a first order approximation, a mid-ocean ridge can be assumed to be a typical place for the generation of such signatures (Sun and McDonough, 1989; Niu and Batiza, 1997). The highly enriched trace elements found in the OIB-type (Fig. 8) are

commonly found in magmas that originated at oceanic islands (Weaver et al., 1987; Sun and McDonough, 1989). However, such geochemical signatures are also known to develop, though less commonly, in subduction zones (Gill and Whelan, 1989; Hole et al., 1995; Leat et al., 2004; Hickey-Vargas et al., 2006). The production of enriched melts (OIB-type and E-MORB-type) can be envisioned to operate in a similar manner to those from mid-ocean ridges (Niu and Batiza, 1997). The enriched melt generation may occur by melting easily fusible, enriched recycled domains within a heterogeneous mantle. The initial and/or less diluted melts in this melting regime will be characterized by OIB- and E-MORB-like geochemical signatures due to a lower solidus temperature of the recycled materials (relative to the surrounding depleted, anhydrous peridotite) (Hirschmann and Stolper, 1996). Although such enriched materials can be already present in a back-arc mantle (Allegre and Turcotte, 1986; Niu et al., 1999), a fertile mantle (with enriched domains) can also be introduced into the mantle source region of the subduction zones via slab window, slab tear, and slab rollback. These mechanisms can create passage for a fertile asthenospheric mantle or plume-contaminated mantle to flow into the melting region of arcs and back-arcs. The East Scotia Ridge (South Atlantic), Fiji (Pacific), West Philippine Basin (Pacific), and James Ross Island (Antarctica) are examples of places where these signatures are found in subduction zones (Gill and Whelan, 1989; Hole et al., 1995; Leat et al., 2000; Hickey-Vargas et al., 2006). The fact that in the studied samples the E-MORB- and OIB-like chemical types are volumetrically small supports the hypothesis that the protoliths of the studied samples were generated in an oceanic arc-back-arc system (Figs. 11 and 12).

5.2. Opening and spreading of the Intra-Pontide Ocean

The numerous bodies of ophiolites preserved within the Intra-Pontide suture zone are interpreted as relicts of the northernmost branch of the Neotethys corresponding to the IPO, located between the Sakarya microplate, to the south, and the Eurasian margin, from which the Istanbul-Zonguldak terrane derived, to the north (Göncüoğlu et al., 2014; Tüysüz et al., 2016; Çimen et al., 2018; Frassi et al., 2018). The protoliths of the oceanic crust preserved in the Intra-Pontide suture zone dated using the non-metamorphic units (i.e., ADU and AKM) indicate that the IPO was already opened in the Middle to Late Jurassic time span (Göncüoğlu et al., 2008, 2012, 2014). Most of the relicts of those ophiolites are affected by the HP-LT metamorphic peak conditions during the uppermost Middle Jurassic age (Marroni et al., 2014; Aygül et al., 2016; Çelik et al., 2016). Considering these ages and the ca. 15–20 Ma necessary for the subducted crust to reach the depth required for the HP metamorphism estimated for these units (Okay et al., 1996; Marroni et al., 2014; Aygül et al., 2016; Aygül and Oberhänsli, 2017), the subduction event had to start during the Early Jurassic. As a consequence, the oldest metaophiolites can be regarded as older than the Early Jurassic (Fig. 12b and c). Palaeontological ages collected in the slide blocks of cherts in the AKM (Göncüoğlu et al., 2008, 2014) corroborate this hypothesis. In these slide blocks, in fact, the oldest ages range from the Middle-Late Anisian to early Norian, which clearly indicate that the IPO, or its margins, reached the deep-water conditions at least in the Late Triassic.

The stratigraphic log of the Sakarya terrane in Central Anatolia (Okay and Tüysüz, 1999) indicate that in the western portion of the terrane, the youngest age of the HP-LT metamorphism is the latest Triassic (Okay and Monié, 1997), whereas the youngest limestones interlayers in the clastic deposits from the Karakaya Complex (Hodul Unit) are Rhaetian in age (Okay and Altıner, 2004). In addition, the Karakaya Complex is unconformably topped by Early Jurassic terrigenous to shallow marine clastic deposits (Kocyigit et al., 1991). Analogously, the stratigraphic log of the Istanbul-Zonguldak terrane is characterized by Middle Triassic deposits unconformably covered by Middle-Late Jurassic conglomerates (Bürnük Formation) and Late Jurassic-Lower Cretaceous shallow-water carbonates (İnaltı Formation) with a gap ranging from the Middle Triassic to Late Jurassic. These stratigraphic settings and the related unconformities have been interpreted by Moix et al. (2008) as being related to uplift and fault-controlled tectonics in the Sakarya and Istanbul-Zonguldak margins resulting from a rifting event and the subsequent opening of an oceanic area.

A detailed evaluation of the local geological data, however, suggests that neither the stratigraphic settings nor the succession of important geological events on Sakarya and Eurasian margins are correlatable. For the Palaeozoic basements, in contrast to the well-developed Atlantic-type Cambrian-Late Carboniferous platform margin of the Eurasian margin, the basement of the Sakarya microplate was characterized by metabasic and metasedimentary rocks intruded by arc-type granitoids of the Devonian and Carboniferous age (Ustaömer et al., 2012) disconformably overlain by a small Permian carbonate platform (Göncüoğlu et al., 2004). Permian and Triassic successions in the Eurasian margin are represented by terrigenous clastics and shallow marine limestones, respectively. The Late Permian granitoids intruding the Eurasian margin are of back-arc-type, attributed to the northward subduction of a Late Palaeozoic oceanic lithosphere (Palaeotethys) (Aysal et al., 2018). In the Sakarya terrane, the Permo-Triassic units (Karakaya Complex *s.l.*) are completely different and include supra-subduction type ophiolites of the Permian age (Topüz et al., 2018), plume-type basalts of the Middle Triassic age (Sayit and Göncüoğlu, 2013), and HP-LT metamorphosed mélanges of the Late Triassic age tectonically interleaved with Late Triassic fore-deep-type sediments (Sayit et al., 2011). The recent geographical distribution of the Karakaya Complex in the Sakarya

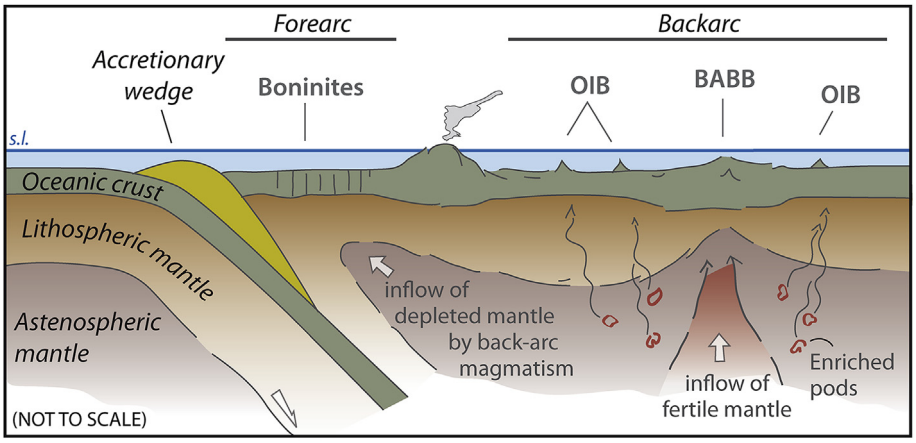

Fig. 11. Simplified idealized petrogenetic model illustrating the occurrence of different types of basalts in a supra-subduction setting. OIB: oceanic island basalt; BABB: back-arc basin basalt.

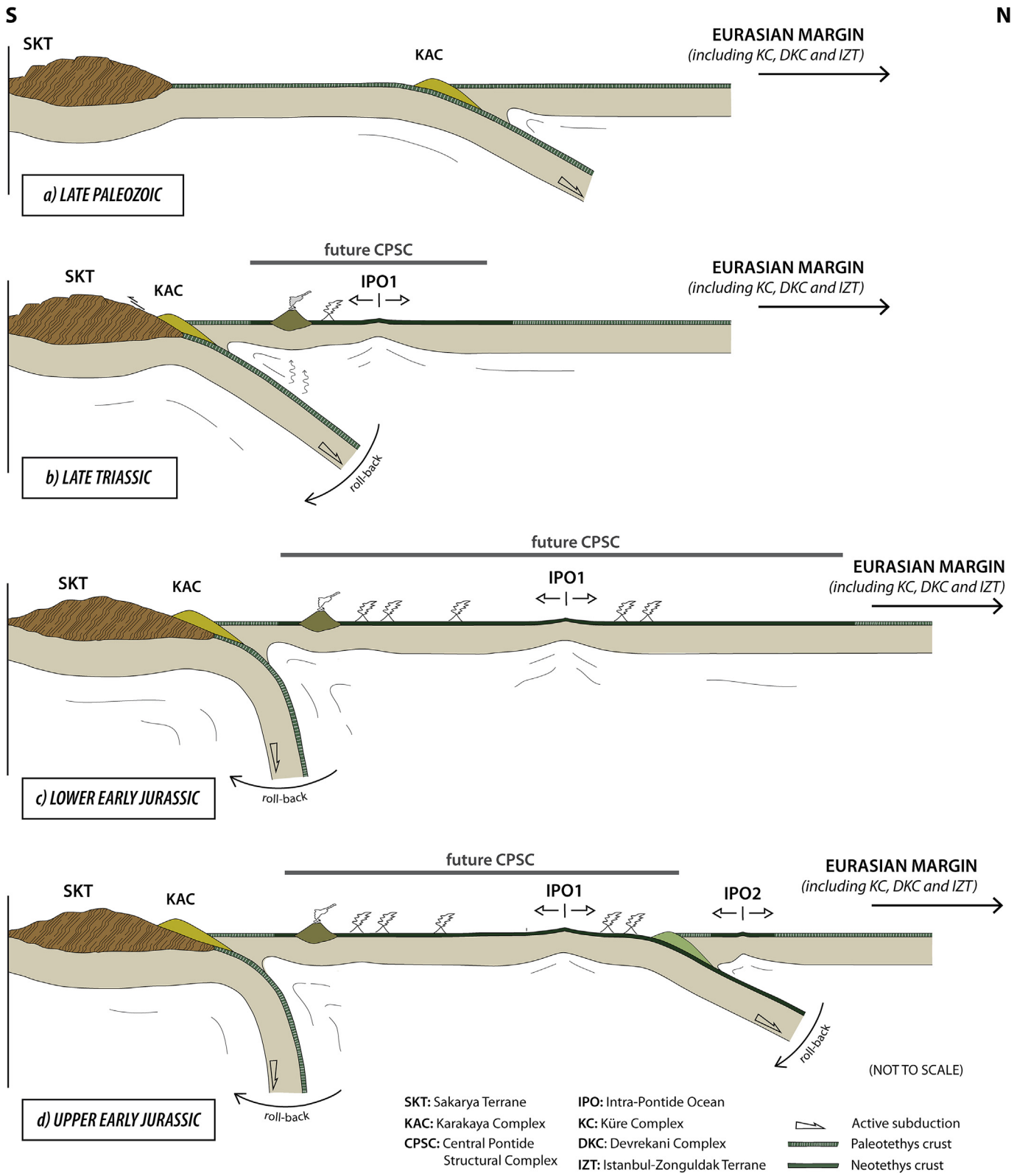

Fig. 12. 2D cartoon showing the tectonic evolution of the Sakarya terrane, IPO and the Istanbul-Zonguldak terrane from the Late Triassic to Late Cretaceous. See text for further explanations.

terrane (Topüz et al., 2018), as well as the south-verging tectonic relations of the oceanic assemblages, indicates their derivation from north of the Sakarya terrane.

By these differences, the Sakarya and the Eurasian margins can hardly represent the conjugates margins of a rift that subsequently resulted in opening of an oceanic area as proposed by Moix et al. (2008). In contrast, the data provided above clearly suggests the presence of a Late Palaeozoic ocean between the active margin of the Sakarya microplate and the

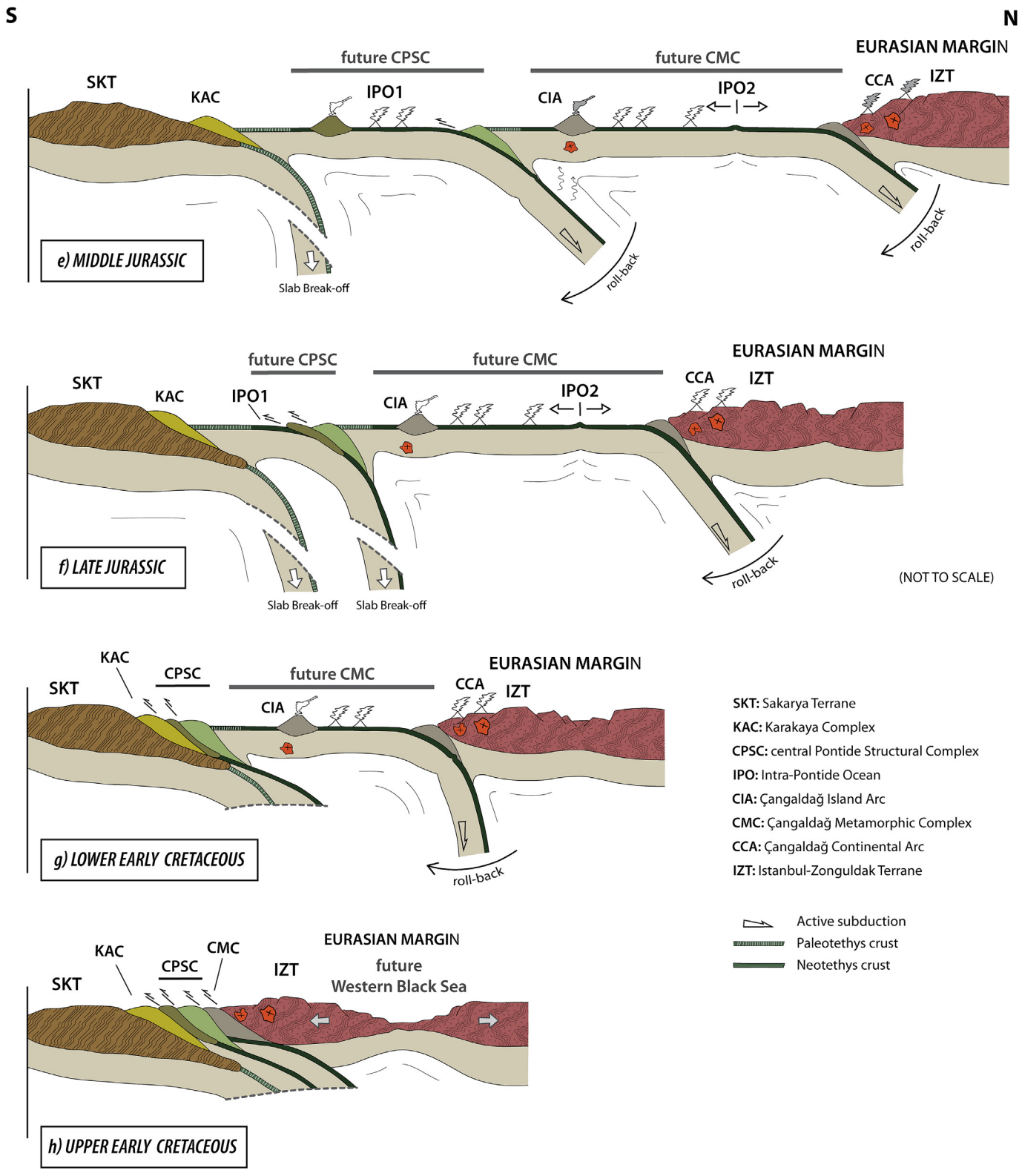

Fig. 12. (*continued*).

passive margin of the Eurasian margin. Its oceanic lithosphere was very probably consumed partly during the Late Triassic by a subduction (probably started during the Late Palaeozoic) and generated the Karakaya Complex (Fig. 12a). However, this intra-oceanic subduction has also created a new supra-subduction-type oceanic lithosphere between the Sakarya and Eurasian margins. According to this picture, the opening of the IPO can be regarded as Late Triassic in age (Fig. 12b and c).

This geodynamic approach contrasts with other palaeogeographic reconstructions for this time-interval (Stampfli and Borel, 2002; Stampfli and Kozur, 2006; Moix et al., 2008; Barrier et al., 2018; Okay et al., 2018) in regard to the position and/or subduction polarity of the pre-Late Triassic Tethys (Palaeotethys). These authors located the Palaeotethys to the south of the Sakarya microplate (Stampfli, 2000; Moix et al., 2008; Okay et al., 2017), whereas others suggest a location between the

Sakarya microplate and the Eurasian plate (Şengör et al., 1982; Yilmaz, 1990; Göncüoğlu et al., 2000; Sayit and Göncüoğlu, 2013; Marroni et al., 2014; Aysal et al., 2018; Çimen et al., 2018). In this study, we prefer the latter model due to the discussion above and because no Late Palaeozoic–Early Triassic oceanic assemblage has been reported yet from the south of the Sakarya terrane that may represent a "Palaeotethys sensu Stampfli (2000)". The Palaeotethys in this study (initially proposed by Göncüoğlu et al., 1997) also differs from the model of Şengör and Yilmaz (1981) and Şengör et al. (1984), where the "Palaeo-Tethys" was located between the Istanbul-Zonguldak microplate and the Eurasian plate.

Our alternative model (Fig. 12) suggests that in this Late Palaeozoic–Early Triassic Palaeotethys Ocean, the oceanic lithosphere starts to subduct to the north to create an accretionary wedge (Karakaya Complex, Okay and Göncüoğlu, 2004). While the Karakaya Complex emplaces to the south onto the Variscan Basement of the Sakarya microplate (Cimmerian event of Şengör and Yilmaz, 1981), the northward subducting slab creates a number of supra-subduction basins on the remnant Palaeotethyan oceanic crust.

This picture clearly implies that the initial IPO opened in a supra-subduction position in respect of the northward subduction of the Palaeotethyan oceanic lithosphere (Fig. 12b and c). Moreover, all the metaophiolites from DDU, SKU and DZU show a geochemical signature indicative of their origin in a supra-subduction setting (Fig. 11), i.e., an oceanic arc-basin system (Sayit et al., 2016; Çelik et al., 2018). Thus, the spreading of the IPO as result of the rollback that affects the northward dipping subduction of the Palaeotethyan oceanic domain is proposed (Fig. 12). In this frame, a discussion whether the Küre Complex is the equivalent of the Sakarya terrane as shown in previous studies (Göncüoglu, 2010) and whether it is generated in relation to the Palaeotethys or IPO is avoided because this is an extremely controversial issue that exceeds the scope of this study. We therefore have used the non-genetic term Eurasian margin (Fig. 12) that includes the Istanbul-Zonguldak terrane, Küre Complex and the Devrekani Metamorphics, which were accreted prior to the early Late Jurassic.

5.3. Closure of the Intra-Pontide Ocean and the configuration of the convergent setting

The evidence for the closure of the IPO is provided by the blueschist and eclogite facies metamorphism detected in the metaophiolites of DDU, SKU and DZU of the Central Pontides Structural Complex. This HP-LT metamorphism is classically interpreted as produced within an accretionary wedge developed above a subducted oceanic crust. The present-day setting of these units consists of an assemblage of highly deformed and metamorphic slices that can be interpreted as subduction tectonic mélanges (Festa et al., 2010, 2012). All these units consist of slices of oceanic lithosphere that, as observed in the modern and fossil accretionary wedges (Moore and Sample, 1986; Meneghini et al., 2009; Monié and Agard, 2009), were underthrust along the subduction zone, accreted at the base of the wedge and exhumed within it (Cloos and Shreve, 1988; Guillot et al., 2009). This mélange is characterized by an HP metamorphism indicating an accretion at depth ranging from approximately 30–35 km for the DDU (Frassi et al., 2018) and SKU to 80 km for the DZU (Marroni et al., 2014; Aygül and Oberhänsli, 2017). According to Frassi et al. (2018) for the DDU, Marroni et al. (2014) for the SKU and Aygül et al. (2016) for the DZU, the oldest ages of the subduction-related metamorphism can be assigned at the boundary between the Middle and Late Jurassic (Fig. 12). As previously stated, the subduction event probably started in the upper Early Jurassic time. This picture implies that since the upper Early Jurassic, the IPO was affected by a subduction that divided it in two different basins, both floored by oceanic crust (hereafter defined as IPO1 and IPO2; see Fig. 12d). The southernmost IPO1 (lower plate), which was located north of the Sakarya plate, was progressively destroyed by a north dipping subduction. In contrast, the northernmost IPO2 (upper plate), which was located south of the Eurasian continental margin, was produced as a result of the subduction rollback (Fig. 12d) and was floored by trapped Palaeotethyan oceanic crust (sensu Karig, 1982). This new oceanic lithosphere is represented by Middle to Late Jurassic ophiolites, like those from the ADU, that are characterized by a clear back-arc geochemical signature (Göncüoğlu et al., 2008, 2012, 2014).

The IPO1 and IPO2 were closed in different times (Fig. 12). The DDU, SKU and DZU, derived from the IPO1, are characterized by a metamorphic retrograde path with a relevant increase of T and concomitant decrease of P (Frassi et al., 2018) (Fig. 10) that is indicative of an exhumation during the continental collision stage (Li, 2014). This exhumation occurred during the Albian to Cenomanian time span for the DDU according to the dating by Okay et al. (2013) and Aygül et al. (2016), whereas for the DZU the available dating (Okay et al., 2006; Aygül et al., 2016) indicates that the exhumation occurred in the Aptian to Turonian time span. No data are available for the exhumation of the SKU. Thus, the IPO1 was probably closed during the lower Early Cretaceous when the Sakarya continental crust was deeply involved in the subduction zone (Fig. 12g).

In this picture, we suggest that the consumption of the IPO2 started when the portion of IPO1 characterized by anomalous crust, i.e., the mid-oceanic ridge or an area floored by oceanic island volcanoes, is involved in the subduction (Fig. 12e and f). This event produced a decrease in the slab retreat rate and a consequent inception of compression in the still open oceanic areas, thus producing a north-dipping subduction in the IPO2 close to the Eurasian continental margin. In this picture, the high-grade amphibolite facies metamorphism detected in the SKU can be a proof of the involvement of a mid-oceanic ridge in the subduction. The inception of the subduction can be regarded as Middle Jurassic in age according to the age of the arc magmatism found at the northern rim of the IPO, like those recognized in the Çangaldağ Continental Arc (Çimen et al., 2017). Different from the IPO1, the IPO2 seemed to remain open throughout the lower Early Cretaceous (Göncüoğlu et al., 2014) and was characterized as an oceanic arc since the Middle Jurassic (i.e., Çangaldağ island arc; Fig. 12e–g).

In our reconstruction, the closure of the IPO2 along the north-dipping subduction zone close to the Eurasian continental margin (Fig. 12f–h) is coherent with the rifting stage that resulted in the opening of the western Black Sea in the Cenomanian (Okay et al., 2013; Nikishin et al., 2015a,b). Moreover, during the late stage of the closure of the IPO2, a new accretionary wedge preserving relict of the Çangaldağ island arc was built-up leading to deformation of the Çangaldağ Metamorphic Complex (Çimen et al., 2017, Figs. 2 and 12h). At the same time, the oceanic lithosphere of IPO2, today represented by the ADU, was obducted southward onto the structure resulting from the collision of the Sakarya continental margin with the accretionary wedge (Göncüoğlu et al., 2014) where the HP metamorphic units were already exhumed at the upper structural levels, as reconstructed for instance for the DDU (Frassi et al., 2018). During the latest stage of the southward emplacement of the ADU, the late Santonian AKM was deposited in a basin along the Sakarya continental margin in front of a composite tectonic stack made up of oceanic- and continental-derived units (Göncüoğlu et al., 2014; Çelik et al., 2016). This picture fits very well with the Barremian to Cenomanian age of the turbidites of Çağlayan Fm (Aygül et al., 2015), which are reported as unconformable deposits at the top of northernmost units of the Intra-Pontide suture zone and the Eurasian continental margin.

5.4. Fate of the ophiolites during the continental collision

Like in worldwide collisional belts, the continental collision follows the end of the subduction of an oceanic crust and consists in the suturing of two paired continental margins (Jamieson and Beaumont, 2013). The result of this process is the building of an orogenic wedge that consists of an imbricate stack of oceanic and continental units variably deformed and metamorphosed.

This picture can also be proposed for the Intra-Pontide suture zone in Central Anatolia, where the orogenic wedge derived from the upper Early

Cretaceous–Early Palaeocene collision between the Istanbul-Zonguldak microplate and the Eurasian continental margins crops out (Fig. 3).

The upper Early Cretaceous–Early Palaeocene continental collision mainly produced the detachment of the Central Pontides Structural Complex and its southward thrusting over the Sakarya terrane simultaneously with the southward translation of the Istanbul-Zonguldak terrane. An orogenic wedge (i.e., Central Pontides Structural Complex) topped by the Istanbul-Zonguldak terrane is consistent with the results of the provenance analyses conducted on the early Maastrichtian - Middle Palaeocene foredeep deposits of the Taraklı Flysch (Catanzariti et al., 2013; Di Rosa et al., 2019) located in front of the orogenic wedge advancing onto the Sakarya continental margin.

In addition, a tectonic history dominated by a southward sense of shear is fully supported by the deformations features related to continental collision identified in the Central Pontides Structural Complex (Frassi et al., 2016, 2018). During the late stage of the continental collision, slices of lower, Sakarya terrane, and upper, Istanbul-Zonguldak terrane, can be incorporated within the orogenic wedge and coupled with the Central Pontides Structural Complex. In our reconstruction, the Geme and Devrekani Complexes represent slices of the Eurasian margin that during the continental collision were detached from their basement and then deformed and imbricated. Analogously, the Kösedağ and Tafano Units, characterized by sequences representative of oceanic and thinned continental volcanic arcs, respectively, can be regarded as detached from their original position and imbricated with the AKM (Ellero et al., 2015b). In our model, the exact location of the Kösedağ arc magmatism is not well constrained, whereas the magmatic rocks as recognized in the Tafano Unit may have been derived from the late stage of closure of the Izmir-Ankara-Erzincan Ocean located south of the Sakarya domain.

At the end of the Palaeocene, the deformations related to continental collision ended and the resulting large-scale structures are sealed since the Late Palaeocene by the inter-mountain deposits (Özcan et al., 2007). Subsequently, since the Early Eocene, the inception of NASZ tectonics deeply modified the previous tectonic setting (Ottria et al., 2017).

6. Summary

Magmatic, structural and metamorphic features of the ophiolites preserved in the DDU, SKU, DZU, ADU and AKM of the Central Pontides Structural Complex provide useful information to reconstruct the geodynamic evolution of the northernmost branch of the Neotethys (i.e., the IPO) during the Mesozoic. The oldest branch of the IPO (i.e., IPO1) opened in the Late Triassic between the Sakarya and the Eurasian continental margins in a supra-subduction setting as a consequence of the rollback of the north-dipping intra-oceanic subduction of the Palaeotethyan oceanic lithosphere.

The spreading of IPO1continued until the Early Jurassic, when a new intraoceanic north-dipping subduction started. The rollback of this subduction slab produced a second Neotethyan oceanic basin (IPO2; represented by the ophiolites of the ADU) characterized by trapped oceanic crust and floored by supra-subduction-type oceanic crust.

Since the Early Jurassic, slices of the IPO1 (i.e., ophiolites preserved in the DDU, SKU, DZU) were accreted at depth at the base of the accretionary wedge and finally exhumed within it during the Late Jurassic-Early Cretaceous. As a consequence of this subduction, a Middle Jurassic arc developed on the Eurasian continental margin and into the IPO2.

The IPO1 and IPO2 were closed at different times. The IPO1 was closed during the lower Early Cretaceous, whereas the IPO2 started to be consumed since the Middle Jurassic when the thickened oceanic domain floored by island arc volcanoes was involved in the subduction of the IPO1. The closure of the IPO2 probably occurred in the upper Early Cretaceous, when the oceanic lithosphere of IPO2 was obducted southward onto the structure resulting from the accretion of the accretionary wedge to the Sakarya continental margin.

The continental collision between Sakarya terrane and the Eurasian margin started during the upper Early Cretaceous and produced the detachment of the Central Pontides Structural Complex and its southward thrusting over the Sakarya terrane simultaneously with the southward translation of the Istanbul-Zonguldak terrane. At the end of Palaeocene, the deformations related to continental collision seemed to stop and the resulting large-scale structures were sealed by Late Palaeocene deposits of the inter-mountain basin and modified by the NASZ tectonics, thus achieving the present-day tectonic features.

Acknowledgements

This research was supported by the Darius Project, PRIN 2008 and PRIN 2010-11 projects (resp. M. Marroni) and PRA 2018 from Università di Pisa. We thank the four anonymous reviewers and Emilio Saccani (Guest Editor) for their careful and constructive review of the paper.

Appendix A. Supplementary data

Supplementary data to this article can be found online at https://doi.org/10.1016/j.gsf.2019.05.010.

References

Akbayram, K., Okay, A.I., Satır, M., 2013. Early Cretaceous closure of the intra-Pontide ocean in western Pontides (northwestern Turkey). Journal of Geodynamics 65, 38–55.

Allegre, C.J., Turcotte, D.L., 1986. Implications of a 2-component marble- cake mantle. Nature 323, 123–127.

Alparslan, G., Dilek, Y., 2017. Seafloor spreading structure, geochronology, and tectonic evolution of the Küre ophiolite, Turkey: a Jurassic continental backarc basin oceanic lithosphere in southern Eurasia. Lithosphere 10, 14–34.

Altiner, D., Koçyiğit, A., Farinacci, A., Nicosia, U., Conti, M.A., 1991. Jurassic, Lower Cretaceous stratigraphy and paleogeographic evolution of the southern part of northwestern Anatolia. Geologica Romana 28, 13–80.

Aydın, M., Demir, O., Özçelik, Y., Terzioğlu, N., Satir, M., 1995. A geological revision of Inebolu, Devrekani Agülı and Küre areas: new observations in PaleoTethys – NeoTethys sedimentary successions. In: Erler, A., Ercan, T., Bingöl, E., Örçen, S. (Eds.), Geology of the Black Sea Region. Maden Tetkik ve Arama Enstitüsü, Ankara, pp. 33–38.

Aygül, M., Oberhänsli, R., 2017. Tectonic stacking of HP/LT metamorphic rocks in accretionary wedges and the role of shallowing slab-mantle decoupling. Tectonics 36. https://doi.org/10.1002/2017TC004689.

Aygül, M., Okay, A.I., Oberhänsli, R., Schmidt, A., Sudo, M., 2015. Late Cretaceous infant intra-oceanic arc volcanism, the Central Pontides, Turkey: petrogenetic and tectonic implications. Journal of Asian Earth Sciences 111, 312–327.

Aygül, M., Okay, A.I., Oberhänsli, R., Sudo, M., 2016. Pre-collisional accretionary growth of the southern Laurasian margin, Central Pontides, Turkey. Tectonophysics 671, 218–234.

Aysal, N., Şahin, S.Y., Güngör, Y., Peytcheva, I., Öngen, S., 2018. Middle Permian–early Triassic magmatism in the western Pontides, NW Turkey: geodynamic significance for the evolution of the paleo-tethys. Journal of Asian Earth Sciences 164, 83–103.

Barrier, E., Vrielynck, B., Brouillet, J.F., Brunet, M.F., Angiolini, L., Kaveh, F., Poisson, A., Pourteau, A., Plunder, A., Robertson, A., Shekawat, R., Sosson, M., Zanchi, A., 2018. - Paleotectonic Reconstruction of the Central Tethyan Realm. Tectonono-Sedimentary-Palinspastic Maps from Late Permian to Pliocene. CCGM/CGMW, Paris. Atlas of 20 maps (scale: 1:15 000 000). http://www.ccgm.org.

Bédard, J.H., 1999. Petrogenesis of boninites from the Betts Cove ophiolite, Newfoundland, Canada: identification of subducted source components. Journal of Petrology 40, 1853–1889.

Berber, F., Göncüoğlu, M.C., Sayit, K., 2014. Geochemistry and tectonic significance of the Kösedağ metavolcanic rocks from the Sakarya Zone, Northern Turkey. Buletini i Shkencave Gjeologjike Issue 2/2014. In: Begiraj, A., et al. (Eds.), Proceedings 20. CBGA Congress.24-26 Sept 2014 Tirana, pp. 161–163.

Berber, F., Göncüoğlu, M.C., Sayıt, K., Crowley, Q., 2016. Geochemistry, Geochronology and Petrology of the Kösedağ Metavolcanic Rocks to the South of Tosya (Central Pontides) In: Proceedings 69th. Geological Congress of Turkey, pp. 266–267.

Bortolotti, V., Principi, G., 2005. Tethyan ophiolites and Pangea breakup. Island Arc 14, 442–470.

Bortolotti, V., Chiari, M., Marroni, M., Pandolfi, L., Principi, G., Saccani, E., 2013. Geodynamic evolution of the ophiolites from Albania and Greece (Dinaric-Hellenic belt): one, two or more oceanic basins? International Journal of Earth Sciences 102, 738–811.

Bortolotti, V., Chiari, M., Göncüoğlu, M.C., Principi, G., Saccani, E., Tekin, U.K., Tassarini, R., 2018. The Jurassic–Early Cretaceous basalt–chert association in the ophiolites of the Ankara Mélange east of Ankara, Turkey: age and geochemistry. Geological Magazine 155, 451–478.

Çakir, Ü., Genç, Y., Paktunç, D., 2006. Intrusive lherzolites within the basalts of Küre ophiolite (Turkey): an occurrence in the Tethyan supra-subduction marginal basin. Geological Journal 41, 123–143.

Çakır, Ü., 2009. Structural and geochronological relationships of metamorphic soles of eastern Mediterranean ophiolites to surrounding units: indicators of intraoceanic subduction and emplacement. International Geological Review 51, 189–215.
Cameron, W.E., McCulloch, M.T., Walker, D.A., 1983. Boninite petrogenesis: chemical and Nd-Sr isotopic constraints. Earth and Planetary Science Letters 65, 75–89.
Catanzariti, R., Ellero, A., Göncüoğlu, M.C., Marroni, M., Ottria, G., Pandolfi, L., 2013. The Taraklı Flysch in the Boyalı area (Sakarya terrane, northern Turkey): implications for the tectonic history of the intrapontide suture zone. C.R. Geosciences 345, 454–461.
Çelik, Ö.F., Chiaradia, M., Marzoli, A., Özkan, M., Billor, Z., Topuz, G., 2016. Jurassic metabasic rocks in the Kızılırmak accretionary complex (Kargı region, Central Pontides, Northern Turkey). Tectonophysics 672–673, 34–49.
Çelik, Ö.F., Marzoli, A., Marschik, R., Chiaradia, M., Mathur, R., 2018. Geochemical, mineralogical and Re-Os isotopic constraints on the origin of Tethyan oceanic mantle and crustal rocks from the Central Pontides, northern Turkey. Mineralogy and Petrology 112, 25–44.
Çimen, O., Göncüoğlu, M.C., Sayit, K., 2016. Geochemistry of the metavolcanic rocks from the Çangaldağ complex in the central Pontides: implications for the middle Jurassic arc-back-arc system in the neotethyan intra-Pontide ocean. Turkish Journal of Earth Sciences 25, 491–512.
Çimen, O., Göncüoğlu, M.C., Simonetti, A., Sayıt, K., 2017. Whole rock geochemistry, zircon U-Pb and Hf isotope systematics of the Çangaldağ pluton: evidences for middle Jurassic Continental Arc magmatism in the central Pontides, Turkey. Lithos 290, 136–158.
Çimen, O., Göncüoglu, M.C., Simonetti, A., Sayıt, K., 2018. New zircon U-Pb LA-ICP-MS ages and Hf isotope data from the Central Pontides: geological and geodynamic constraints. Journal of Geodynamics 116, 23–36.
Cloos, M., Shreve, R.L., 1988. Subduction-channel model of prism accretion, mélange formation, sediment subduction, and subduction erosion at convergent plate margins: 1. Background and description. Pure and Applied Geophysics 128, 455–500.
Cohen, K.M., Finney, S.C., Gibbard, P.L., Fan, J.-X., 2013. The ICS international chronostratigraphic chart. Episodes 36, 199–204.
Çolakoğlu, A.R., Sayit, K., Günay, K., Göncüoğlu, M.C., 2012. Geochemistry of mafic dykes from the Southeast Anatolian ophiolites, Turkey: implications for an intra-oceanic arc-basin system. Lithos 132–133, 113–126.
Derman, A.S., Sayili, A., 1995. Inaltı formation: a key unit for regional geology. In: Erler, A., Ercan, T., Bingöl, E., Örçen, S. (Eds.), Geology of the Black Sea Region. Maden Tetkik ve Arama Enstitüsü, Ankara, pp. 104–108.
Di Rosa, M., Farina, F., Marroni, M., Pandolfi, L., Göncüoglu, M.C., Ellero, A., Ottria, G., 2019. U-Pb zircon geochronology of intrusive rocks from an exotic block in the Late Cretaceous - Paleocene Tarakli Flysch (northern Turkey): constraints on the tectonics of the Intrapontide suture zone. Journal of Asian Earth Sciences 171, 277–288.
Dilek, Y., Moores, E.M., 1990. Regional tectonics of the eastern Mediterranean ophiolites. In: Malpas, J., Moores, E., Panayiotou, A., Xenophontos, C. (Eds.), Ophiolites, Oceanic Crustal Analogues: Proceedings of the Symposium "Troodos 1987", Geological Survey Department, Nicosia (1990), pp. 295–309.
Dilek, Y., Thy, P., Hacker, B., Grundvig, S., 1999. Structure and petrology of Tauride ophiolites and mafic dike intrusions (Turkey): implications for the Neo-Tethyan ocean. The Geological Society of America Bulletin 111, 1192–1216.
Ellero, A., Ottria, G., Marroni, M., Pandolfi, L., Göncüoğlu, M.C., 2015a. Analysis of the North Anatolian Shear Zone in Central Pontides (northern Turkey): insight for geometries and kinematics of deformation structures in a transpressional zone. Journal of Structural Geology 72, 124–141.
Ellero, A., Ottria, G., Sayit, K., Catanzariti, C., Frassi, C., Göncüoğlu, M.C., Marroni, M., Pandolfi, L., 2015b. Geological and geochemical evidence for a Late Cretaceous continental arc in the Central Pontides, northern Turkey. Ofioliti 40, 73–90.
Elmas, A., Yiğitbaş, E., 2001. Ophiolite emplacement by strike-slip tectonics between the Pontide zone and the Sakarya zone in north-western Anatolia, Turkey. International Journal of Earth Sciences 90, 257–269.
Festa, A., Pini, G.A., Dilek, Y., Codegone, G., 2010. Mélanges and mélange-forming processes: a historical overview and new concepts. International Geology Review 52 (10–12), 1040–1105.
Festa, A., Dilek, Y., Pini, G.A., Codegone, G., Ogata, K., 2012. Mechanisms and processes of stratal disruption and mixing in the development of mélanges and broken formations: redefining and classifying mélanges. Tectonophysics 568, 7–24.
Frassi, C., Göncüoğlu, M.C., Marroni, M., Pandolfi, L., Ruffini, L., Ellero, A., Ottria, G., Sayit, K., 2016. The intra-pontide suture zone in the Tosya-Kastamonu area, northern Turkey (with geological map at 1:50.000 scale). Journal of Maps 12, 211–219. https://doi.org/10.1080/17445647.2016.1192330.
Frassi, C., Marroni, M., Pandolfi, L., Göncüoğlu, M.C., Ellero, A., Ottria, G., Sayit, K., McDonald, C.S., Balestrieri, M.L., Malasoma, A., 2018. Burial and exhumation history of the Daday Unit (Central Pontides, Turkey): implications for the closure of the Intra-Pontide oceanic basin. Geological Magazine 155, 356–376.
Fretzdorff, S., Livermore, R.A., Devey, C.W., Leat, P.T., Stoffers, P., 2002. Petrogenesis of the back-arc East Scotia ridge, South Atlantic ocean. Journal of Petrology 43, 1435–1467.
Frost, B.R., Frost, C.D., 2013. Essentials of Igneous and Metamorphic Petrology. Cambridge University Press, p. 314.
Gill, J.B., Whelan, P., 1989. Post subduction ocean island alkali basalts in Fiji. Journal of Geophysical Research 94, 4579–4588. https://doi.org/10.1029/JB094iB04p04579.
Göncüoğlu, M.C., 2010. Introduction to the Geology of Turkey: Geodynamic Evolution of the Pre-Alpine and Alpine Terranes. MTA, pp. 1–69.
Göncüoğlu, M.C., 2011. Geology of the Kütahya-Bolkardağ belt. Min. Res. Explor. Bull. 142, 223–277.
Göncüoğlu, M.C., Erendil, M., 1990. Pre-late cretaceous tectonic units of the Armutlu peninsula. In: Proceedings of 8th Turkish Petroleum Congress, vol. 8, pp. 161–168.
Göncüoğlu, M.C., Erendil, M., Tekeli, O., Aksay, A., Kuşçu, A., Ürgün, B., 1987. Geology of the Armutlu peninsula. IGCP-5 Guide Book, 5, pp. 12–18.
Göncüoğlu, M.C., Kozlu, H., Dirik, K., 1997. Pre-Alpine and Alpine terranes in Turkey: explanatory notes to the terrane map of Turkey. Ann Geol Pays Helleniques 37, 515–536.
Göncüoğlu, M.C., Turhan, N., Senturk, K., Ozcan, A., Uysal, S., 2000. A geotraverse across NW Turkey: tectonic units of the Central Sakarya region and their tectonic evolution. In: Bozkurt, E., Winchester, J., Piper, J.A. (Eds.), Tectonics and Magmatism in Turkey and the Surrounding Area, vol. 173. Geological Society of London, Special Publications, pp. 139–161.
Göncüoğlu, M.C., Turhan, N., Tekin, K., 2003. Evidence for the Triassic rifting and opening of the neotethyan Izmir-Ankara ocean, northern edge of the Tauride-Anatolide platform, Turkey. Bull. Geol. Soc. Italy, Special Volume 2, 203–212.
Göncüoğlu, M.C., Kuwahara, K., Tekin, U.K., Turhan, N., 2004. Upper Permian (Changxingian) Radiolarian Cherts within the Clastic Successions of the. Turkish Journal of Earth Sciences 13 (2), 201–213.
Göncüoğlu, M.C., Gürsu, S., Tekin, U.K., Koksal, S., 2008. New data on the evolution of the Neotethyan oceanic branches in Turkey: late Jurassic ridge spreading in the Intra-Pontide branch. Ofioliti 33, 153–164.
Göncüoğlu, M.C., Sayit, K., Tekin, U.K., 2010. Oceanization of the northern Neotethys: geochemical evidence from ophiolitic mélange basalts within the Izmir–Ankara suture belt, NW Turkey. Lithos 116, 175–187.
Göncüoğlu, M.C., Marroni, M., Sayit, K., Tekin, U.K., Ottria, G., Pandolfi, L., Ellero, A., 2012. The Ayli Dag ophiolite sequence (central-northern Turkey): a fragment of middle Jurassic oceanic lithosphere within the Intra-Pontide suture zone. Ofioliti 37, 77–91.
Göncüoğlu, M.C., Marroni, M., Pandolfi, L., Ellero, A., Ottria, G., Catanzariti, R., Tekin, U.K., Sayit, K., 2014. The Arkot Dağ Mélange in Araç area, central Turkey: evidence of its origin within the geodynamic evolution of the Intra-Pontide suture zone. Journal of Asian Earth Sciences 85, 117–139.
Göncüoğlu, M.C., Tekin, U.K., Sayit, K., Bedi, Y., Uzuncimen, S., 2015. Opening, evolution and closure of the Neotethyan oceanic branches in Anatolia as inferred by radiolarian research. Radiolaria 35, 88–90.
Görür, N., Monod, O., Okay, A.I., Sengör, A.M.C., Tüysüz, O., Yiğitbaş, E., Sakinc, M., Akkök, R., 1997. Palaeogeographic and tectonic position of the Carboniferous rocks of the western Pontides (Turkey) in the frame of the Variscan belt. Bulletin de la Societe Geologique de France 168, 197–205.
Guillot, S., Hattori, K., Agard, P., Schwartz, S., Vidal, O., 2009. Exhumation processes in oceanic and continental subduction contexts: a review. In: Subduction Zone Geodynamics. Springer, Berlin, Heidelberg, pp. 175–205.
Harris, N.B.W., Kelley, S., Okay, A.I., 1994. Post-collision magmatism and tectonics in northwest Anatolia. Contributions to Mineralogy and Petrology 117, 241–252.
Hässig, M., Rolland, Y., Sosson, M., Galoyan, G., Sahakyan, L., Topuz, G., Çelik, Ö.F., Avagyan, A., Müller, C., 2013. Linking the NE Anatolian and Lesser Caucasus ophiolites: evidence for large-scale obduction of oceanic crust and implications for the formation of the Lesser Caucasus-Pontides Arc. Geodinamica Acta 26, 311–330.
Hickey-Vargas, R., Savov, I.P., Bizimis, M., Ishii, T., Fujioka, K., 2006. Origin of diverse geochemical signatures in igneous rocks from the West Philippine Basin: implications for tectonic models. In: Christie, D. (Ed.), Back-Arc Spreading Systems: Geological, Biological, Chemical and Physical Interactions, vol. 166. AGU Geophysical Monograph Series, pp. 287–303.
Hippolyte, J.-C., Müller, C., Kaymakçi, N., Sangu, E., 2010. Dating of the Black Sea basin: new nannoplankton ages from its inverted margin in the central Pontides (Turkey). In: Stephenson, R.A., Kaymakci, N., Sosson, M., Starostenko, V., Bergerat, F. (Eds.), Sedimentary Basin Tectonics from the Black Sea and Caucasus to the Arabian Platform, vol. 340. Geological Society, London, Sp. Publ, pp. 113–136. https://doi.org/10.1144/SP340.7.
Hirschmann, M., Stolper, E., 1996. A possible role for garnet pyroxenite in the origin of the "garnet signature". In: MORB, Contributions to Mineralogy and Petrology, vol. 124, pp. 185–208.
Hole, M.J., Saunders, A.D., Rogers, G., Sykes, M.A., 1995. The relationship between alkaline magmatism, lithospheric extension and slab window formation along continental destructive plate margins. In: Smellie, J.L. (Ed.), Volcanism Associated with Extension at Consuming Plate Margins, vol. 81. Geological Society Special Publications, pp. 265–285.
Jamieson, R.A., Beaumont, C., 2013. On the origin of orogens. GSA Bull 125, 1671–1702. https://doi.org/10.1130/B30855.1.
Karig, D.E., 1982. Accreted terranes in the northern part of the Philippine archipelago. In: Balce, G.R., Zanoria, A.s. (Eds.), Geology and Tectonics of the Luzon-Marianas Region, vol. 1. Philippines SEATAR Committee (Spec. Pub.), pp. 1–243.
Kocyigit, A., Altiner, D., Farinacci, A., Nicosia, U., Conti, M.A., 1991. Late Triassic–Aptian evolution of the Sakarya divergent margin: implications for the opening history of the Northern Neo-tethys, in the north-western Anatolia, Turkey. Geologica Romana 27, 81–101.
Kozur, H., Aydin, M., Demir, O., Yakar, H., Göncüoğlu, M.C., Kuru, F., 2000. New stratigraphic and palaeogeographic results from the Palaeozoic and early Mesozoic of the Middle Pontides (northern Turkey) in the Azdavay, Devrekani, Küre and İnebolu areas. Implications for the Carboniferous-Early Cretaceous geodynamic evolution and some related remarks to the Karakaya oceanic rift basin. Geologica Croatica 53, 209–268.
Leat, P.T., Livermore, R.A., Millar, I.L., Pearce, J.A., 2000. Magma supply in back-arc spreading centre segment E2, East Scotia Ridge. Journal of Petrology 41, 845–866.
Leat, P.T., Pearce, J.A., Barker, P.F., Millar, I.L., Barry, T.L., Larter, R.D., 2004. Magma genesis and mantle flow at a subducting slab edge: the South Sandwich arc-basin system. Earth and Planetary Science Letters 227, 17–35.

Li, Z., 2014. A review on the numerical geodynamic modeling of continental subduction, collision and exhumation. Science China Earth Sciences 57, 47–69.
Malpas, J., Zhou, M.F., Robinson, P.T., Reynolds, P.H., 2003. Geochemical and geochronological constraints on the origin and emplacement of the Yarlung Zangbo ophiolites, Southern Tibet. In: Dilek, Y., Robinson, P.T. (Eds.), Ophiolites in Earth History, vol. 218. Geological Society, London, Special Publications, pp. 191–206.
Marroni, M., Frassi, C., Göncüoğlu, M.C., Di Vincenzo, G., Pandolfi, L., Rebay, G., Ellero, A., Ottria, G., 2014. Late Jurassic amphibolite-facies metamorphism in the intra-pontide suture zone (Turkey): an eastward extension of the Vardar ocean from the Balkans into Anatolia? Journal of the Geological Society 171, 605–608.
Meneghini, F., Marroni, M., Moore, J.C., Pandolfi, L., Rowe, C.D., 2009. The processes of underthrusting and underplating in the geologic record: structural diversity between the Franciscan complex (California), the Kodiak complex (Alaska) and the internal Ligurian units (Italy). Geological Journal 44, 126–152.
Moix, P., Beccaletto, L., Kozur, H.W., Hochard, C., Rosselet, F., Stampfli, G.M., 2008. A new classification of the Turkish terranes and sutures and its implication for the paleotectonic history of the region. Tectonophysics 451, 7–39. https://doi.org/10.1016/j.tecto.2007.11.044.
Monie, P., Agard, P., 2009. Coeval blueschist exhumation along thousands of kilometers: implications for subduction channel processes. Geochemistry, Geophysics, Geosystems 10 (7), Q07002.
Moore, J.C., Sample, J., 1986. Mechanisms of subduction accretion: recognition in the stratigraphic record. Memorie della Societa Geologica Italiana 31, 107–118.
Nikishin, A.M., Okay, A.I., Tüysüz, O., Demirer, A., Wannier, M., Amelin, N., Petrov, E., 2015a. The Black Sea basins structure and history: new model based on new deep penetration regional seismic data. Part 2: tectonic history and paleogeography. Marine and Petroleum Geology 59, 656–670.
Nikishin, A.M., Okay, A.I., Tüysüz, O., Demirer, A., Amelin, N., Petrov, E., 2015b. The Black Sea basins structure and history: new model based on new deep penetration regional seismic data. Part 1: basins structure and fill. Marine and Petroleum Geology 59, 638–655.
Niu, Y., Batiza, R., 1997. Trace element evidence from seamounts for recycled oceanic crust in the Eastern Pacific mantle. Earth and Planetary Science Letters 148, 471–483.
Niu, Y.L., Collerson, K.D., Batiza, R., Wendt, I., Regelous, M., 1999. Origin of enriched-type mid-ocean ridge basalt at ridges far from mantle plumes: the East Pacific Rise at 11°20′N. Journal of Geophysical Research 104 (B4), 7067–7087.
Okay, A.I., 1989. Tectonic units and sutures in the Pontides, northern Turkey. In: Sengör, A.M.C. (Ed.), Tectonic Evolution of the Tethyan Region. Kluwer Academic Publishers, pp. 109–116.
Okay, A.I., 2000. Was the Late Triassic orogeny in Turkey caused by the collision of an oceanic plateau?. In: Bozkurt, E., Winchester, J.A., Piper, J.D.A. (Eds.), Tectonic and Magmatism in Turkey and Surrounding Area, vol. 173. Geological Society of London, Special Publications, pp. 25–41.
Okay, A.I., Altiner, D., 2004. Uppermost Triassic limestone in the Karakaya Complex-stratigraphic and tectonic significance. Turkish Journal of Earth Sciences 13 (2), 187–199.
Okay, A.I., Göncüoğlu, M.C., 2004. Karakaya Complex: a review of data and concepts. Turkish Journal of Earth Sciences 13, 77–95.
Okay, A.I., Monié, P., 1997. Early Mesozoic subduction in the eastern Mediterranean: evidence from Triassic eclogite in northwest Turkey. Geology 25, 595–598.
Okay, A.I., Topuz, G., 2017. Variscan orogeny in the Black Sea region. International Journal of Earth Sciences 106, 569–592.
Okay, A.I., Tüysüz, O., 1999. Tethyan sutures of northern Turkey. In: Durand, B., Jolivet, L., Horvath, F., Seranne, M. (Eds.), Tethyan Sutures of Northern Turkey, vol. 156. Geological Society, London, Special Publications, pp. 475–515.
Okay, A.I., Whitney, D.L., 2011. Blueschists, eclogites, ophiolites and suture zones in northwest Turkey: a review and a field excursion guide. Ofioliti 35, 131–172.
Okay, A.I., Satır, M., Maluski, H., Siyako, M., Monié, P., Metzger, R., Akyüz, S., 1996. Palaeo- and Neo-Tethyan events in northwest Turkey. In: Yin, E., Harrison, M. (Eds.), Tectonics of Asia. University Press, Cambridge, pp. 420–441.
Okay, A.I., Monod, O., Monié, P., 2002. Triassic blueschists and eclogites from Northwest Turkey: vestiges of the Paleo-Tethyan subduction. Lithos 64, 155–178.
Okay, A.I., Satır, M., Siebel, W., 2006. Pre-alpide Palaeozoic and Mesozoic orogenic events in the eastern Mediterranean region. In: Gee, D.G., Stepherson, R.A. (Eds.), European Lithosphere Dynamics, vol. 32. Geological Society London, pp. 389–406 (Memoirs).
Okay, A.I., Sunal, G., Sherlock, S., Altiner, D., Tüysüz, O., Kylander-Clark, A.R.C., Aygül, M., 2013. Early Cretaceous sedimentation and orogeny on the southern active margin of Eurasia: central Pontides, Turkey. Tectonics 32, 1247–1271.
Okay, A.I., Sunal, G., Tüysüz, O., Sherlock, S., Keskin, M., Kylander-Clark, A.R.C., 2014. Low-pressure– high temperature metamorphism during extension in a Jurassic magmatic arc, Central Pontides, Turkey. Journal of Metamorphic Geology 32, 49–69.
Okay, A.I., Altiner, D., Kiliç, A.M., 2015. Triassic limestone, turbidites and serpentinite–the Cimmeride orogeny in the Central Pontides. Geological Magazine 152, 460–479.
Okay, A.I., Altiner, D., Sunal, G., Aygül, M., Akdoğan, R., Altiner, S., Simmons, M., 2017. Geological evolution of the central Pontides. In: Simmons, M.D., Tari, G., Okay, A.I. (Eds.), Petroleum Geology of the Black Sea, vol. 464. Geological Society, London, Special Publications. https://doi.org/10.1144/SP464.3.
Okay, A.I., Altiner, D., Sunal, G., Aygül, M., Akdoğan, R., Altiner, S., Simmons, M., 2018. Geological evolution of the Central Pontides. Geological Society, London, Special Publications, 464(1), 33–67.
Okuyucu, C., Dimitrova, T.K., Göncüoğlu, M.C., Gedik, I., 2017. Late Permian (Tatarian) fluvio-lacustrine successions in NW Anatolia (Zonguldak terrane, Turkey): palaeogeographic implications. Geological Magazine 154, 1073–1087.
Önder, F., Boztuğ, D., Yılmaz, O., 1987. New paleontological data (conodont) from the lower Mesozoic rocks of the Göynükdağı-Kastamonu region at the western Pontides, Turkey. In: Melih Tokay Geology Semposium, Abstracts, pp. 127–128.
Önen, A.P., 2003. Neotethyan ophiolitic rocks of the Anatolides of NW Turkey and comparison with Tauride ophiolites. Journal of the Geological Society 160, 947–962.
Ottria, G., Pandolfi, L., Catanzariti, R., Da Prato, S., Ellero, A., Frassi, C., Göncüoğlu, M.C., 2017. Evolution of an early Eocene pull-apart basin in the central Pontides (northern Turkey): new insights into the origin of the north Anatolian shear zone. Terra Nova 29, 392–400.
Özcan, E., Less, G., Kertesz, B., 2007. Late Ypresian to middle Lutetian Orthophragminid record from central and northern Turkey: Taxonomy and remarks on zonal scheme. Turkish Journal of Earth Sciences 16, 281–318.
Parlak, O., Robertson, A., 2004. The ophiolite-related Mersin Mélange, southern Turkey: its role in the tectonic-sedimentary setting of Tethys in the Eastern Mediterranean region. Geological Magazine 141, 257–286.
Parlak, O., Rizaoglu, T., Bagci, U., Karaoglan, F., Hoeck, V., 2009. Geochemistry of ophiolites inthe Southeast Anatolia, Turkey. Tectonophysics 473, 173–187.
Parlak, O.F., Karaoğlan, Rızaoğlu, T., Klötzli, U., Koller, F., Billor, Z., 2013. U–Pb and 40Ar– 39Ar geochr onology of the ophiolites and granitoids from the Tauride belt: implications for the evolution of the Inner Tauride suture. Journal of Geodynamics 65, 22–37.
Pearce, J.A., 1996. A users guide to basalt discrimination diagrams. In: Wyman, D.A. (Ed.), Trace Element Geochemistry of Volcanic Rocks: Applications for Massive Sulphide Exploration. Geological Association of Canada, Short Course Notes, vol. 12, pp. 79–113.
Pearce, J.A., Peate, D.W., 1995. Tectonic implications of the composition of volcanic arc magmas. Annual Review of Earth and Planetary Sciences 23, 251–286.
Pilet, S., Hernandez, J., Sylvester, P., Poujol, M., 2005. The metasomatic alternative for ocean island basalt chemical heterogeneity. Earth and Planetary Science Letters 236, 148–166.
Plunder, A., Agard, P., Chopin, C., Okay, A.I., 2013. Geodynamics of the Tavşanlı zone, western Turkey: insights into subduction/obduction processes. Tectonophysics 608, 884–903.
Rizaoğlu, T., Parlak, O., Höck, V., Koller, F., Hames, W.E., Billor, Z., 2009. Andean type active margin formation in the Eastern Taurides: geochemical and geochronological evidence from the Baskil Granitoid, SE Turkey. Tectonophysics 473, 188–207.
Robertson, A.H.F., 2002. Overview of the genesis and emplacement of Mesozoic ophiolites in the eastern Mediterranean Tethyan region. Lithos 65, 1–67.
Robertson, A.H.F., 2012. Late Palaeozoic–Cenozoic tectonic development of Greece and Albania in the context of alternative reconstructions of Tethys in the Eastern Mediterranean region. International Geology Review 54, 373–454.
Robertson, A.H.F., Dixon, J.E., 1984. Introduction: aspects of the geological evolution of the Eastern Mediterranean. In: Dixon, J.E., Robertson, A.H.F. (Eds.), The Geological Evolution of the Eastern Mediterranean, vol. 17. Geological Society of London Special Publications, pp. 1–74.
Robertson, A.H.F., Ustaömer, T., 2004. Tectonic evolution of the intra-pontide suture zone in the Armutlu peninsula, NW Turkey. Tectonophysics 381, 175–209.
Robertson, A.H.F., Ustaömer, T., 2011. Role of tectonic-sedimentary mélange and Permian–Triassic cover units, central southern Turkey in Tethyan continental margin evolution. Journal of Asian Earth Sciences 40, 98–120.
Robertson, A.H.F., Ustaömer, T., 2012. Testing alter-native tectono-stratigraphic interpretations of the Late Palaeozoic-Early Mesozoic Karakaya complex in NW Turkey: support for an accretionary origin related to northward subduction of Palaeotethys. Turkish Journal of Earth Sciences 21, 961–1007.
Robertson, A.H.F., Ustaömer, T., Pickett, E.A., Collins, A.S., Andrew, T., Dixon, J.E., 2004. Testing models of Late Palaeozoic–Early Mesozoic orogeny in Western Turkey: support for an evolving open-Tethys model. Journal of the Geological Society 161, 501–511.
Robertson, A., Parlak, O., Ustaömer, T., Taslı, K., Inan, N., Dumitrica, P., Karaoglan, F., 2013. Subduction, ophiolite genesis and collision history of Tethys adjacent to the Eurasian continental margin: new evidence from the Eastern Pontides, Turkey. Geodinamica Acta 26, 230–293.
Robertson, A., Parlak, O., Ustaömer, T., Taslı, K., İnan, N., Dumitrica, P., Karaoğlan, F., 2014. Subduction, ophiolite genesis and collision history of Tethys adjacent to the Eurasian continental margin: new evidence from the Eastern Pontides, Turkey. Geodinamica Acta 27, 1–64.
Saccani, E., 2015. A new method of discriminating different types of post-Archean ophiolitic basalts and their tectonic significance using Th-Nb and Ce-Dy-Yb systematics. Geoscience Frontiers 6, 481–501.
Savostin, L.A., Sibuet, J.C., Zonenshain, L.P., Le Pichon, X., Roulet, M.J., 1986. Kinematic evolution of the Tethys belt from the Atlantic ocean to the Pamirs since the Triassic. Tectonophysics 123, 1–35.
Sayit, K., 2013. Immobile trace element systematics of ocean island basalts: the role of oceanic lithosphere in creating the geochemical diversity. Ofioliti 38, 101–120.
Sayit, K., Göncüoğlu, M.C., 2013. Geodynamic evolution of the Karakaya Mélange Complex, Turkey: a review of geological and petrological constraints. Journal of Geodynamics 65, 56–65.
Sayit, K., Göncüoğlu, M.C., Furman, T., 2010. Petrological reconstruction of Triassic seamounts/oceanic islands within the Palaeotethys: geochemical implications from the Karakaya subduction/accretion Complex, Northern Turkey. Lithos 119, 501–511.
Sayit, K., Tekin, U.K., Göncüoğlu, M.C., 2011. Early-middle Carnian radiolarian cherts within the Eymir unit, Central Turkey: constraints for the age of the palaeotethyan Karakaya complex. Journal of Asian Earth Sciences 42, 398–407.
Sayit, K., Göncüoğlu, M.C., Tekin, U.K., 2015. Middle Carnian arc-type basalts from the Lycian nappes, Southwestern Anatolia: early late Triassic subduction in the northern branch of Neotethys. The Journal of Geology 123, 561–579.

Sayit, K., Marroni, M., Göncüoğlu, M.C., Pandolfi, L., Ellero, A., Ottria, G., Frassi, C., 2016. Geological setting and geochemical signatures of the mafic rocks from the Intra-Pontide suture zone: implications for the geodynamic reconstruction of the Mesozoic Neotethys. International Journal of Earth Sciences 105, 39–64.

Sayit, K., Bedi, Y., Tekin, U.K., Göncüoğlu, M.C., 2017. Middle Triassic back-arc basalts from the blocks in the Mersin Mélange, southern Turkey: implications for the geodynamic evolution of the northern Neotethys. Lithos 268, 102–113.

Sayıt, K., Göncüoğlu, M.C., 2009. Geochemistry of mafic rocks of the Karakaya complex, Turkey: evidence for plume-involvement in the Palaeotethyan extensional regime during the Middle and Late Triassic. International Journal of Earth Sciences 98, 157–185.

Schmid, S.M., Bernoulli, D., Fügenschuh, B., Matenco, L., Schefer, S., Schuster, R., Tischler, M., Ustaszewski, K., 2008. The Alpine–Carpathian–Dinaridic orogenic system: correlation and evolution of tectonic units. Swiss Journal of Geosciences 101, 139–183.

Searle, M., Cox, J., 1999. Tectonic setting, origin and obduction of the Oman ophiolite. GSA Bulletin 111, 104–122.

Şengör, A.M.C., Yilmaz, Y., 1981. Tethyan evolution of Turkey, a plate tectonic approach. Tectonophysics 75, 181–241.

Şengör, A.M.C., Yilmaz, Y., Ketin, İ., 1982. Remnants of a pre-Late Jurassic Ocean in northern Turkey: fragments of Permian-Triassic Paleo-Tethys?: discussion and reply: reply. GSA Bulletin 93, 932–936.

Şengör, A.M.C., Yılmaz, Y., Sungurlu, O., 1984. Tectonics of the Mediterranean Cimmerides: nature and evolution of the western termination of Palaeo-Tethys. Geological Society, London, Special Publications, 17(1), 77–112.

Şengör, A.M.C., Tüysüz, O., Imren, C., Sakınç, M., Eyidoğan, H., Görür, N., Le Pichon, X., Rangin, C., 2005. The North Anatolian fault: a new look. Annual Review of Earth and Planetary Sciences 33, 37–112.

Stampfli, G.M., 2000. Tethyan oceans. In: Bozkurt, E., Winchester, J., Piper, J.A. (Eds.), Tectonics and Magmatism in Turkey and the Surrounding Area, vol. 173. Geological Society of London, Special Publications, pp. 1–23.

Stampfli, G.M., Borel, G.D., 2002. A plate tectonic model for the Palaeozoic and Mesozoic constrained by dynamic plate boundaries and restored synthetic oceanic isochrones. Earth and Planetary Science Letters 169, 17–33.

Stampfli, G.M., Kozur, H.W., 2006. Europe from the Variscan to the Alpine cycles. In: Gee, D.G., Stephenson, R.A. (Eds.), European Lithosphere Dynamics, vol. 32. Geological Society of London, Memoirs, pp. 57–82.

Sun, S.-S., McDonough, W.F., 1989. Chemical and isotopic systematics of oceanic basalts: implications for mantle composition and processes. In: Saunders, A.D., Norry, M.J. (Eds.), Magmatism in the Ocean Basins, vol. 42. Geological Society, London, Special Publications, pp. 313–345.

Tekin, U.K., Göncüoğlu, M.C., Pandolfi, L., Marroni, M., 2012. Middle-Late Triassic radiolarian cherts from the Arkot Dağ mélange in northern Turkey: implications for the life span of the northern Neotethyan branch. Geodinamica Acta 25, 305–319.

Thuizat, R., Whitechurch, H., Montigny, R., Juteau, T., 1981. K–Ar dating of some intra-ophiolitic metamorphic soles from the East Mediterranean: new evidence for oceanic thrusting before obduction. Earth and Planetary Science Letters 52, 302–310.

Tokay, M., 1973. Geological observations on them North Anatolian fault zone between Gerede and Ilgaz. In: Proceedings of North Anatolian Fault and Earthquakes Symposium. M.T.A. Publ., pp. 12–29

Topüz, G., Candan, O., Zack, T., Yılmaz, A., 2017. East Anatolian plateau constructed over a continental basement: No evidence for the East Anatolian accretionary complex. Geology 45, 791–794.

Topüz, G., Okay, I.A., Schwarz, W.H., Sunal, G., Altherr, R., Kylander-Clark, A.R.C., 2018. A middle Permian ophiolite fragment in Late Triassic greenschist- to blueschist-facies rocks in NW Turkey: an earlier pulse of suprasubduction-zone ophiolite formation in the Tethyan belt. Lithos 300–301, 121–135.

Tüysüz, O., 1990. Tectonic evolution of a part of the Tethyside orogenic collage: the Kargı Massif, northern Turkey. Tectonics 9, 141–160.

Tüysüz, O., 1999. Geology of the cretaceous sedimentary basins of the western Pontides. Geological Journal 34, 75–93.

Tüysüz, O., Yiğitbaş, E., 1994. The Karakaya basin: a Palaeo-Tethyan marginal basin and its age of opening. Acta Geologica Hungarica 37, 327–350.

Tüysüz, O., Melinte-Dobrinescu, M.C., Yılmaz, İ.Ö., Kirici, S., Švabenická, L., Skupien, P., 2016. The Kapanboğazı formation: a key unit for understanding Late Cretaceous evolution of the Pontides, N Turkey. Palaeogeography, Palaeoclimatology, Palaeoecology 441, 565–581.

Ural, M., Arslan, M., Göncüoglu, M.C., Tekin, U.K., Kürüm, S., 2015. Late Cretaceous arc and back-arc formation within the southern Neotethys: whole-rock, trace element and Sr-Nd-Pb isotopic data from basaltic rocks of the Yüksekova Complex (Malatya-Elazig, SE Turkey). Ofioliti 40, 57–72.

Ustaömer, T., Robertson, A.H.F., 1994. Late Paleozoic marginal basin and subduction–accretion: the paleotethyan Küre complex, central Pontides, northern Turkey. Journal of the Geological Society, London 151, 291–305. https://doi.org/10.1144/gsjgs.151.2.0291.

Ustaömer, T., Robertson, A.H.F., 1997. Tectonic-sedimentary evolution of the north-tethyan margin in the central Pontides of northern Turkey. In: Robinson, A.G. (Ed.), Regional and Petroleum Geology of the Black Sea and Surrounding Region, vol. 68. American Association of Petroleum Geologists Memoir, pp. 255–290.

Ustaömer, T., Robertson, A.H.F., 1999. Geochemical evidence used to test alternative plate tectonic models for the pre-Upper Jurassic (Palaeotethyan) units in the Central Pontides, N Turkey. Geological Journal 34, 25–53.

Ustaömer, P.A., Ustaömer, T., Gerdes, A., Robertson, A.H., Collins, A.S., 2012. Evidence of Precambrian sedimentation/magmatism and Cambrian metamorphism in the Bitlis Massif, SE Turkey utilising whole-rock geochemistry and U–Pb LA-ICP-MS zircon dating. Gondwana Research 21 (4), 1001–1018.

van Hinsbergen, D.J.J., Maffione, M., Plunder, A., Kaymakcı, N., Ganerød, M., Hendriks, B.W.H., Corfu, F., Gürer, D., de Gelder, G.I.N.O., Peters, K., McPhee, P.J., Brouwer, F.M., Advokaat, E.L., Vissers, R.L.M., 2016. Tectonic evolution and paleogeography of the Kırşehir Block and the Central Anatolian Ophiolites, Turkey. Tectonics 35, 983–1014. https://doi.org/10.1002/2015TC004018.

Weaver, B.L., Wood, D.A., Tarney, J., Joron, J.L., 1987. Geochemistry of ocean island basalts from the South Atlantic: Ascension, Bouvet, St. Helena, Gough and Tristan da Cunha. Geological Society, London, Special Publications 30, 253–267.

Winchester, J.A., Floyd, P.A., 1977. Geochemical discrimination of different magma series and their differentiation products using immobile elements. Chemical Geology 20, 325–343.

Yalınız, M.K., Floyd, P.A., Göncüoğlu, M.C., 1996. Supra-subduction zone ophiolites of central Anatolia: geochemical evidence from the Sarıkaraman ophiolite, Aksaray, Turkey. Mineralogical Magazine 60, 697–710.

Yilmaz, Y., Genc, S.C., Yiğitbaş, E., Bozcu, M., Yilmaz, K., 1995. Geological evolution of the late Mesozoic continental margin of Northwestern Anatolia. Tectonophysics 243, 155–171.

Yılmaz, Y., 1990. Allochthonous terranes in the Tethyan Middle East, Anatolia and surrounding regions. Philosophical Transactions of the Royal Society A331, 611–624.

Yılmaz, O., Bonhomme, M.G., 1991. K-Ar isotopic age evidence for a Lower to Middle Jurassic low-pressure and a Lower Cretaceous high-pressure metamorphic events in north-central Turkey. Terra Abstracts 3, 501.

Yılmaz, Y., Tüysüz, O., Yiğitbaş, E., Genç, S.C., Şengör, A.M.C., 1997. Geology and tectonic evolution of the Pontides. In: Robinson, A.G. (Ed.), Regional and Petroleum Geology of the Black Sea and Surrounding Region, vol. 68. Bullettin of American Association Petroleum Geology, pp. 183–226.

Zhang, L., Jin, Z., 2016. High-temperature metamorphism of the Yushugou ophiolitic slice: late Devonian subduction of seamount and mid-oceanic ridge in the South Tianshan orogen. Journal of Asian Earth Sciences 132, 75–93.

Zindler, A., Hart, S., 1986. Chemical geodynamics. Annual Review of Earth and Planetary Sciences 14, 493–571.